Politecnico di Torino

Master's degree in Mechanical Engineering
Academic year 2021/2022

Validation of CFD models for jets and plums in fission reactors

Supervisors:

Antonio Froio (DENERG)

Andrea Zappatore (DENERG)

Candidate:

Shovkat Sotivoldiev

Contents

Introduction: Isothermal single jet experiments

The cooling system of nuclear reactor is very important, as the safety of the whole system significantly depends on it. Nowadays, it's design and the design of the fission and fusion power plants depend on the models that can simulate a fluid flow in a given geometry taking into account all the environmental and other conditions. There are variety of models available that are results of different approaches, thus the computational time will also vary depending on the approach. Nevertheless, most of these approaches are based on the Navier-Stokes equations. So having the availability of too many models, only some of them will be implemented to simulate a fluid flow and then verification and validation process will be performed too.

The analysis concerns mostly the fluid flow in an upper plenum of the cooling system. Verification and validation process (V&V) will be implemented on a scaled-down (1/16) version of a High-Temperature reactor which is a benchmark proposed by the ASME V&V Committee in collaboration with the Texas A&M University [1] which is illustrated in the figure 1:

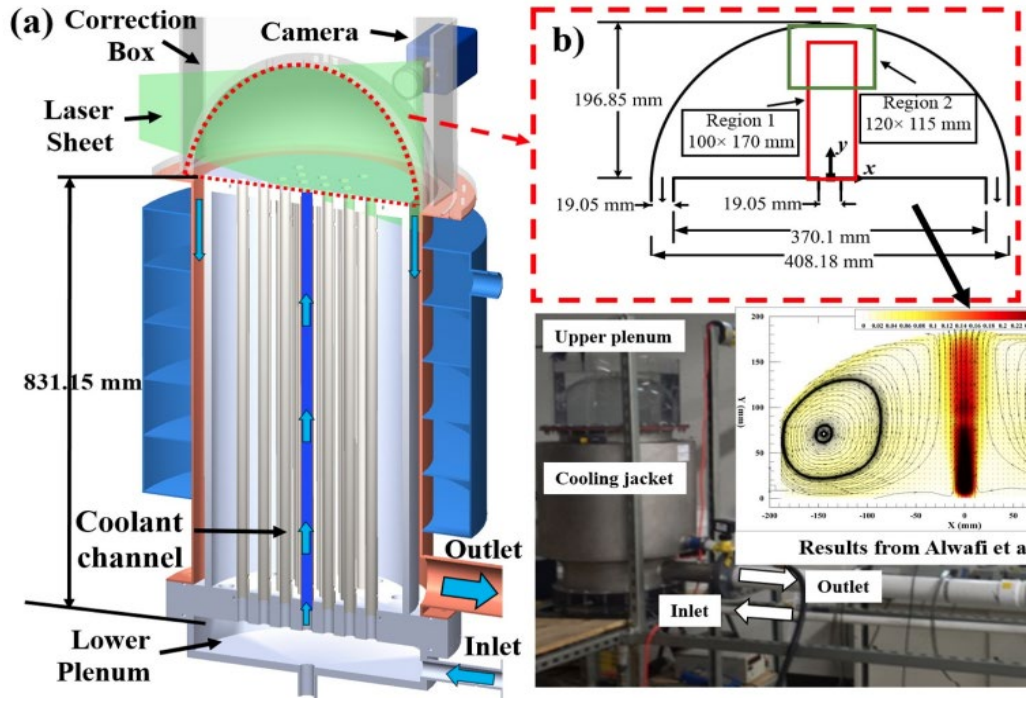

Fig.1: The scheme of the scaled-down (1/16) version of a High-Temperature reactor which is a benchmark proposed by the ASME V&V Committee in collaboration with the Texas A&M University.

The scaling analysis of the test facility has been discussed in Experimental Modeling of VHTR Plenum Flows During Normal Operation and Pressurized Conduction Cooldown, McCreery and Condie (2006) [2]. A brief review of the experimental facility is provided. An overview of the experimental facility, including the facility design with primary components, a flow chart, a sketch of the flow measurement area, and a core layout is illustrated. The test facility is a closed loop, having the main components which are an upper plenum, lower plenum and a core. The core of the real HTGR contains 1020 fuel blocks arranged in a hexagonal shape, while the core of the scaled facility contains only 25 blocks which consist of 25 pipes (diameter Dj = 19.05 mm) to simulate the coolant channels. The coolant channels of the scaled facility were also arranged in the hexagonal shape and into five groups, whose locations were the top (T), bottom (B), right (R), left (L), and center (C).

The goal of this work is to compare the different steady-state and time-dependent models with the experimental results and to note more realistic ones.

The experimental results of velocity profile of turbulent flow is obtained by TR-PIV type of sensors. There are three measurements areas involved in acquisition of the velocity measurements. One measurement area is close to the jet inlet and covers the central part of the facility, while the second is located close to the upper plenum wall and the last one is the largest one, which covers the half of the whole plenum. They cover the areas of 100 × 170 [mm2], 120 × 115 [mm2], and 204 × 197 [mm2] (width × height). We will focus to the measurements obtained by the measurement areas 1, and 2 as they are appropriate to represent isothermal cases.

In this study, the flow characteristics of an isothermal single jet is mixing in the upper plenum and corresponds to five Reynolds numbers ranging from Re1 = 3,413 to Re5 = 12,819 were characterized by the PIV measurements. But the analysis will be focused mostly on the Re1 and Re5. The Reynolds number is the ratio of inertial forces to viscous forces. It is a dimensionless number which categorizes the fluids (from laminar to turbulent).

Using the Star CCM+ Siemens software [3], it's possible to simulate the turbulent fluid flow in the plenum by imposing and comparing different CFD models.

Reynolds-Averaged Navier-Stokes (RANS) models , Large Eddy Simulation (LES) and Direct-Numerical Simulation (DNS) [4] are the most known models in the field of turbulent fluid flow analysis and simulation. DNS is the most accurate approach for simulating turbulent flow as it solves all the turbulent scales in time and space by the Navier-Stokes equations. But DNS requires very large computational time and usually

used over simple geometry or low Re. Therefore, in this thesis work, the RANS and LES models will be compared.

For simulation it's necessary to have a fully-developed flow which can be obtained on the other CCM file by creating a suitable geometry, boundary conditions and physics.

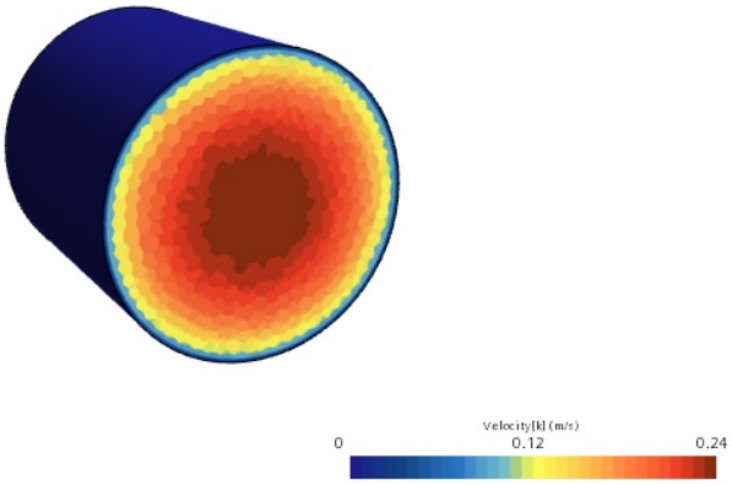

Fig.2: Velocity scene of the geometry for creating a fully-developed flows.

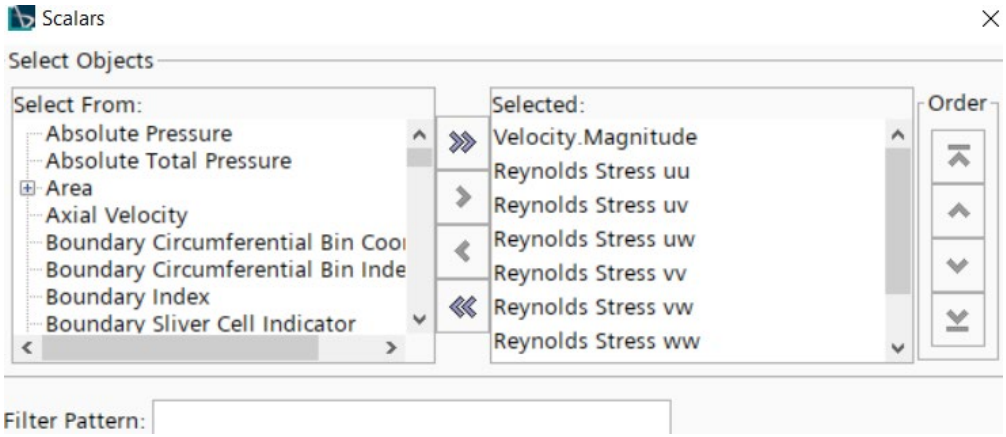

Fig.3: Scalars of the fully-developed flow.

Then the needed data (velocity magnitude, turbulent kinetic energy, Reynolds stresses, turbulent dissipation rate), in a form of table, can be exported and later imported in the main testing CCM file. After that by setting the main model and boundary conditions (fully-developed inlet velocity, outlet pressure, etc) the simulation process can be started.

RANS

The RANS models are very appropriate for time-averaged, steady-state analysis and simulation of the turbulent flows. The main purpose of RANS equations is to split the flow into time-averaged part and fluctuating part, whereby an instantaneous quantity is decomposed into its time-averaged and fluctuating quantities. These models give quite good, approximated results and more importantly, they are not expensive, they don't require large computational time.

Therefore, the different Reynolds-Averaged Navier-Stokes (RANS) models were compared for several flows having the different Reynold's numbers.

2D simulation

Considering the axis-symmetry of the geometry, it is possible to run the 2D simulation which would drastically decrease the computational time in comparison with the one that would be necessary in order to simulate the full 3D model. Obviously, due the several aspects, such as mesh type and size, 2D plane and 3D volume, etc. the results can differ, but the difference should be minimal, therefore 2D simulation will be performed.

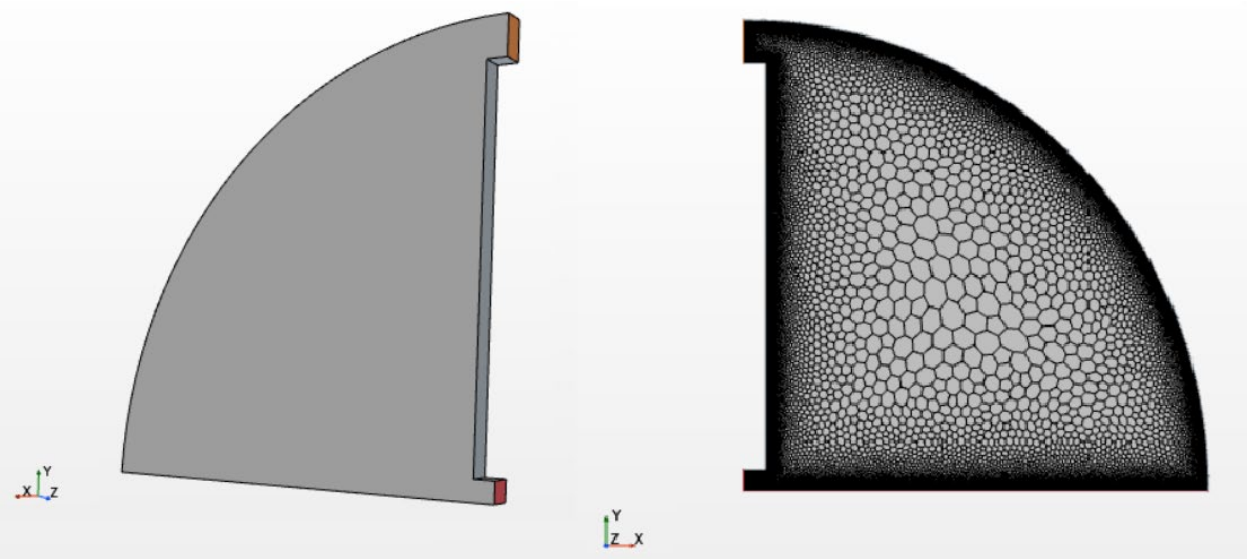

Fig.4 Geometry and mesh scene of the 2D model.

The geometry is for sure not 2D itself, as the fluid inlet conditions, including mass flow rate should be imposed which obviously depends on the cross-section area. But then due to the operation: Badge for 2D meshing it is possible to switch into 2D.

Re=Re1

Re=Re1=3413 (Reynold's number) which is turbulent, where the mass flow rate equals to 0.05kg/s. Knowing the initial data of fluid: mass flow rate, temperature, Reynold's number, viscosity, the physical properties of the fluid can be set in the simulation.

Set	Mass flow rate at the jet inlet [kg/s]	Reynolds number	Averaged inlet temperature [°C]
1	0.05	3,413	19.74
2	0.089	5,963	
3	0.118	7,912	
4	0.158	10,622	
5	0.19	12,819	

Table1: Mass flow rate at the jet inlet, Reynolds numbers, and the averaged inlet temperature for different experimental sets [1].

The several RANS models will be performed and verified which are: K-epsilon Standard [4], K-omega SST [5], Realizable K-epsilon two-layer [6] and Reynolds stresses or Reynolds stress transport (Linear pressure strain) [7].

The K-Epsilon turbulence model is a two-equation model that solves transport equations for the turbulent kinetic energy k and the turbulent dissipation rate ε in order to determine the turbulent eddy viscosity.
Different types of the K-Epsilon model have been in use for a long time and it has been widely used for industrial applications. Since the inception of the K-Epsilon model, there have been many attempts to improve it. The most significant improvements have been incorporated into Simcenter STAR-CCM+.
The two-layer approach allows the K-Epsilon model to be applied in the viscous-affected layer. In this approach, the computation is divided into two layers (near the wall and far from the wall). In the layer next to the wall, the turbulent dissipation rate ε and the turbulent viscosity mu are defined as the functions of wall distance. The values of ε in the near-wall layer are mixed smoothly with the values computed from solving the transport equation far from the wall. The equation for the turbulent kinetic energy is solved across the entire flow domain.
The K-Omega turbulence model is a two-equation model that solves transport equations for the turbulent kinetic energy k and the specific dissipation rate ω (ω is proportional to ε/k) in order to determine the turbulent eddy viscosity.

The comparison at different height levels (1d, 3d, 6d, 9d, where d=19.05mm) is shown on the figures below:

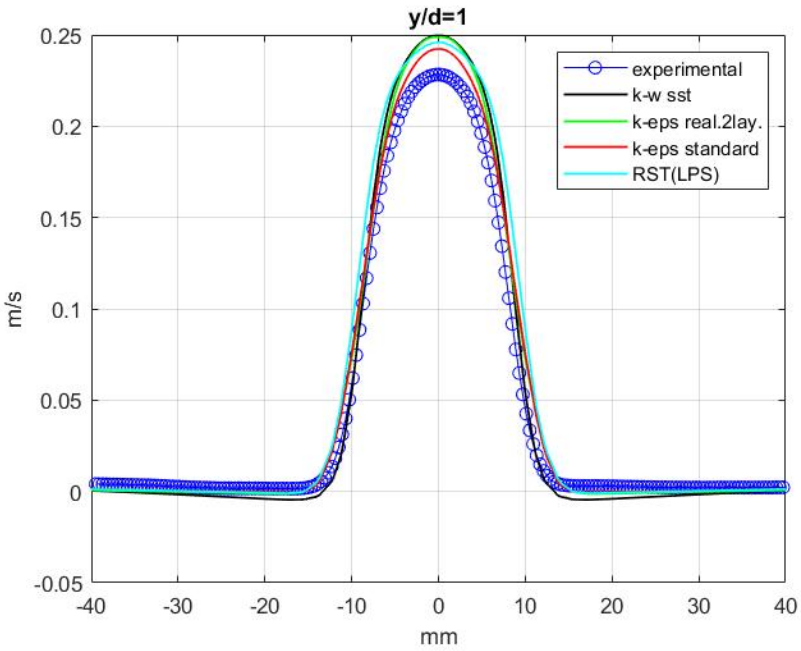

Fig.5: Velocity magnitude of RANS models at y/d=1 (Re1, 2D analysis).

On the cross section at the distance y/d=1 (19.05 mm) all the models were quite precise, but the k-epsilon standard has the best fit among the others. The k-epsilon standard's maximum velocity error is around 6.2%. The value of error comes from a simple equation:

$$Error\% = \frac{max.velocity\ of\ exp.result - max.velocity\ of\ k{-}eps.standard}{max.velocity\ of\ exp.result} * 100\%$$

The velocity profiles are quite sharp because it is very close to the inlet and have a high kinetic energy.

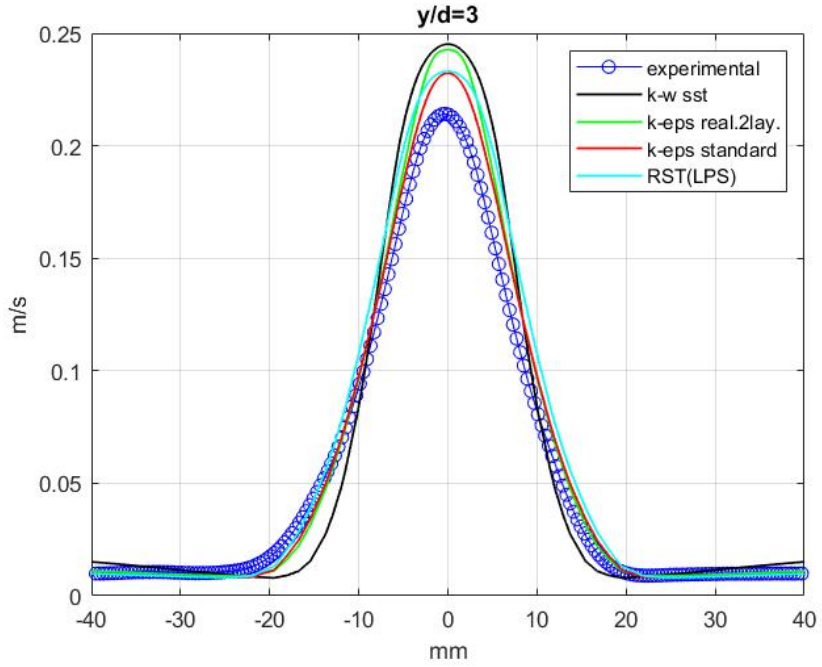

Fig.6: Velocity magnitude of RANS models at y/d=3 (Re1, 2D analysis).

On this graph it's shown the velocity profiles at the distance y/d=3 (57.15 mm). Here the differences of profiles are increased in comparison to y/d=1, but nevertheless models are quite good. As in the previous case the k-epsilon standard and also Reynolds stress transport (Linear pressure strain) models show the best results.

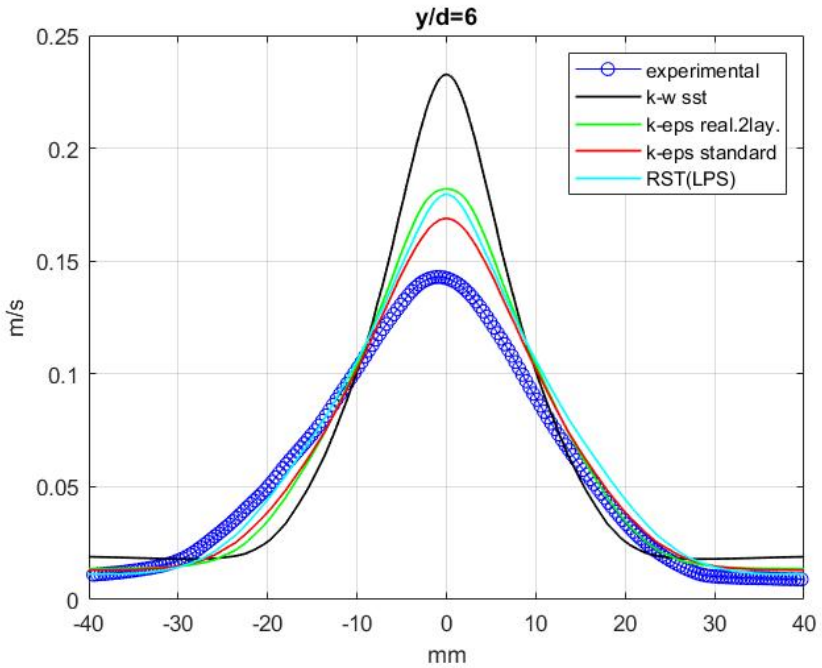

Fig.7: Velocity magnitude of RANS models at y/d=6 (Re1, 2D analysis).

Looking at the figure 7, at this distance, it is obvious that the k-omega sst model is not appropriate anymore as it's velocity magnitude is too high from the actual one and moreover the velocity shape is much sharper, however, the other three models are still suitable.

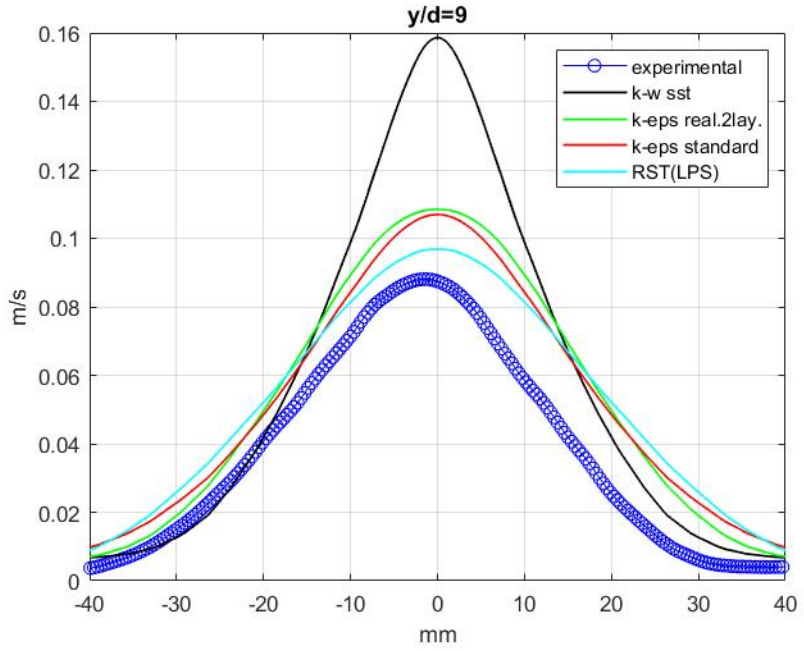

Fig.8: Velocity magnitude of RANS models at y/d=9 (Re1, 2D analysis).

At the distance y/d=9 which is close to the upper plenum, we can notice the smoothness of the velocity profile, the profiles are not as sharp as they were at the lower distances from the inlet. The difference of RANS models are remarkable here. It is clear that the K-omega SST model differs a lot from the actual experimental velocity profile, whereas three other models are quite suitable. The form and shape of both k-epsilon: standard and realizable 2 layer are not so far from the actual one, the difference of velocity vertical component increases in a region closer to the center of the plenum. However, Reynolds stress transport (Linear pressure strain) model shows the best result at this distance.

Finally, also the velocity scenes of the different models can be visually compared which should obviously coincide with the plotted results at the different height levels.

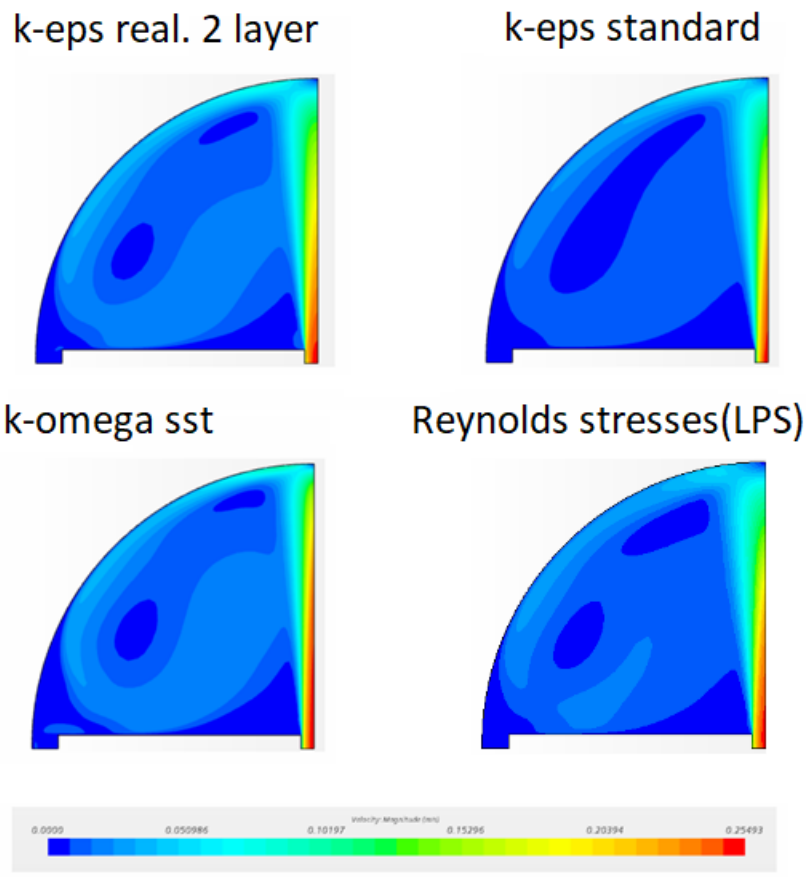

Fig.9: Velocity magnitude scenes of RANS models (Re1, 2D analysis).

Having only the indication of velocity magnitude it is not possible to see the conditions of the velocity in the outlet, but having the outlet cross section much bigger than inlet and , therefore, being concentrated at the velocity profile which is close to inlet, it is noticeable that in K-omega SST velocity scene the velocity is more intense even at higher levels, which coincides with the velocity magnitude plot that were discussed before. Whereas in the three other models the velocity magnitude decreases starting from lower distances, but the area with higher magnitude around the middle is larger.

Re=Re5

Then the same procedure can be done for Re=Re5=12819. Having the same geometry, the same plenum, the mass flow rate increases up to 0.19kg/s. As the cross-section of the pipe is constant, the velocity components and kinetics of the flow are increased. That is why it is necessary to create a new fully-developed fluid with appropriate properties in order to impose it on the inlet boundary condition. Then the simulation should restart.

After obtaining new results and looking at the velocity profiles at the same distances that were considered for Re=Re1, the changes can be noticed. The figures representing the plots are located are discussed below:

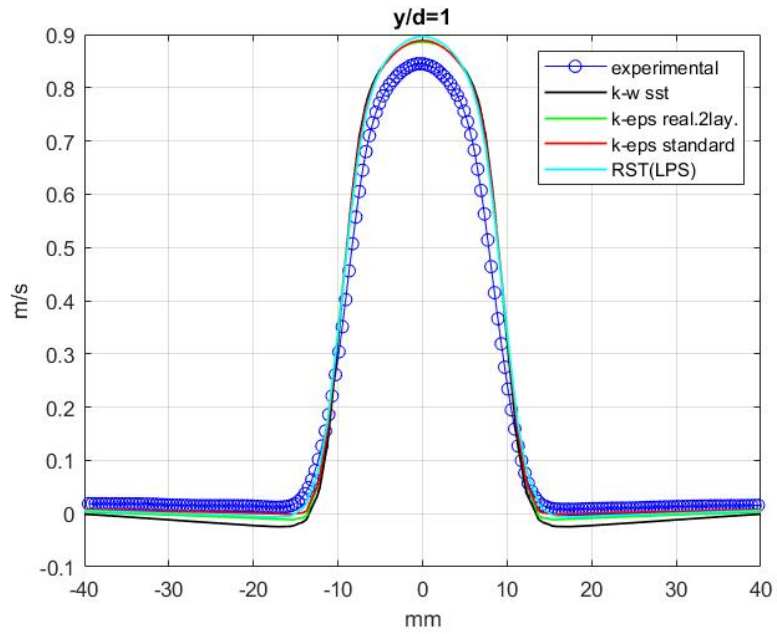

Fig.10: Velocity magnitude of RANS models at y/d=1 (Re5, 2D analysis).

As it was expected the initial velocity at the distance very close to inlet is high and the velocity profile is sharp. All the models are quite precise and almost the same in the range x(-13;13) [mm]. The actual maximum velocity magnitude at the height level, which is only 19.05mm far from inlet, is around 0.84 [m/s], while the numerical maximum velocity is around 0.89 [m/s]. So the error is around 5.7% which is even better than the error occurred at the same level but with Re=Re1. So an increase of the Reynold's number do not always imply an increase of an error, for example in our case at the distance y/d=1, the effect was vice versa, even if the difference was negligible. But for sure this will drastically depend on the y/d distance.

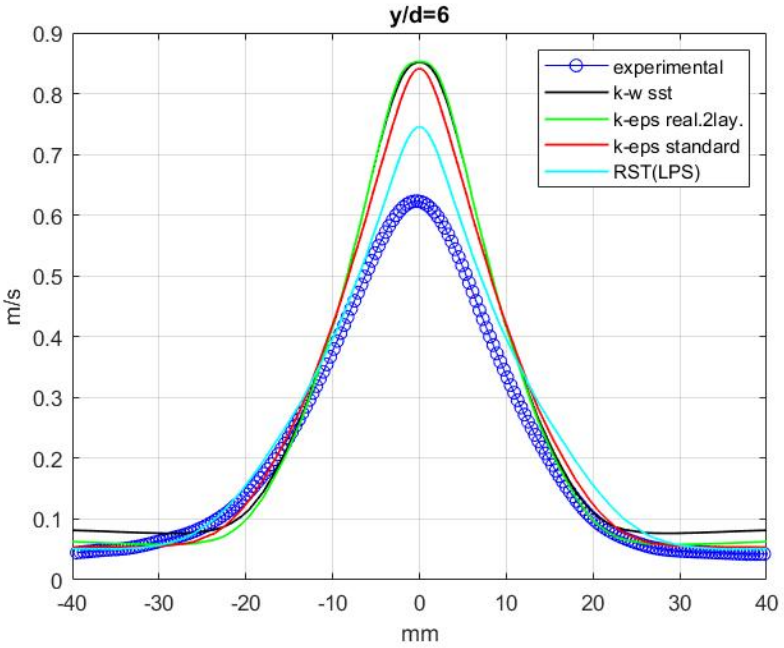

Fig.11: Velocity magnitude of RANS models at y/d=6 (Re5, 2D analysis).

When Re=Re1 was simulated, the results of K-epsilon standard and Realizable K-epsilon 2 layer were good enough at y/d=6, however, now they are as inaccurate as K-omega SST model. Whereas Reynolds stress transport (Linear pressure strain) shows better result.

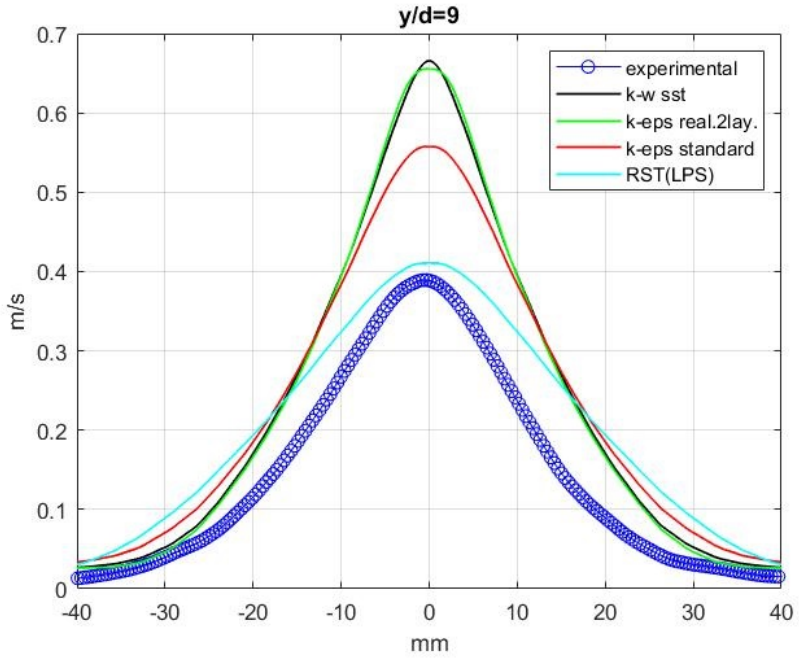

Fig.12: Velocity magnitude of RANS models at y/d=9 (Re5, 2D analysis).

Here, K-epsilon standard model somehow rehabilitates, whereas the two other models (k-omega sst and k-epsilon real. 2 layer) are still inaccurate in the sense of velocity magnitude and also the shape. Reynolds stresses (LPS) model shows a great result even if the shape is slightly differs.

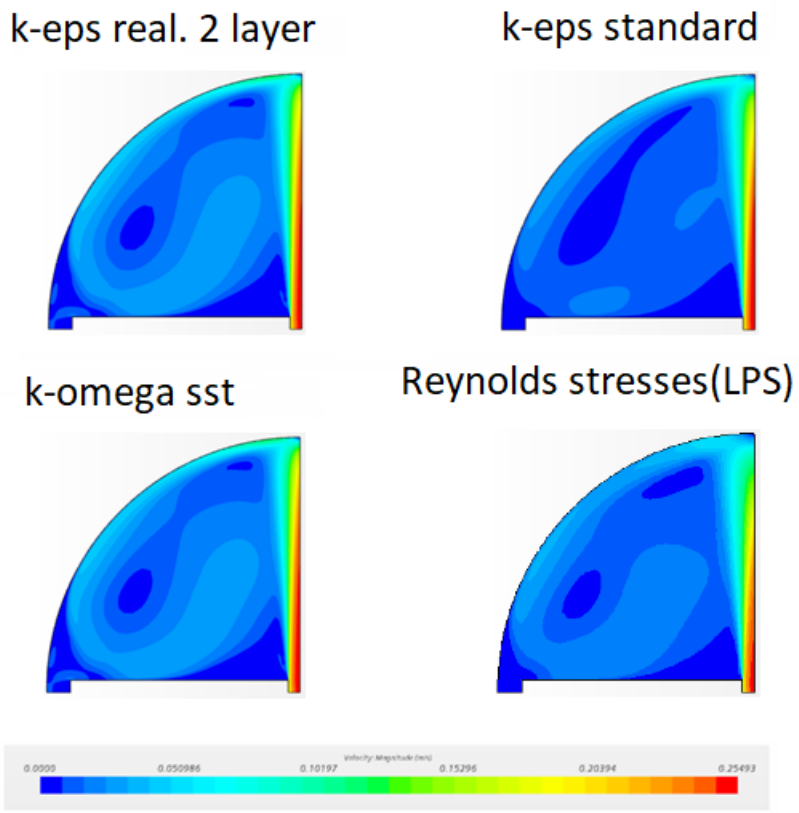

Fig.13: Velocity magnitude scenes of RANS models (Re5, 2D analysis).

Large Eddy Simulation (LES)

LES is a mathematical model for turbulent flow used in computational fluid dynamics. In comparison with “Direct Numerical Simulation” (DNS), this model takes into account mostly non-small length scales in order to decrease the computational time. In comparison to RANS (which is done in steady state condition), LES is performed in implicit unsteady state which means that the process is not averaged in time. This makes the LES more realistic than RANS but increases the computational cost too, thus, the more powerful computers were used for this simulation, otherwise it (computation, simulation) would take much longer time.

The two ways were followed to perform this simulation:

1) 3D Quarter model
2) 3D Full model

The mesh size of the geometry model is very important in LES, because it directly affects the precision of results and a computational time. That is why the “Kolmogorov length scale” and “Taylor micro scale” were identified in order to limit the mesh size between them. There values were around 1 mm (Kolmogorov LS) and 10 mm (Taylor MS) [8].

Also, the time step must be imposed accurately, this is a trade of between good simulation and computational time. The “Convective Courant Number” field function helped to establish the time step (0.001 s). And a maximum inner iterations are set to 15, which means that each millisecond 15 iterations are performed by the software [8]. Taking into account that this is a time dependent model, the velocity profiles in the beginning of the simulation are not very stable.

Considering the computational cost of LES, in order to decrease it (to decrease the time needed for computation), the simulation was initially launched by RANS: Reynolds stress transport (Linear pressure strain or LPS) [7] steady state model just to develop the shape of flow inside the plenum. Then, approximately after 1000 iteration, the model was changed into the LES (WALE Subgrid Scale) [9] by imposing appropriate inlet boundary conditions.

LPS is one of the Reynolds Stress Transport (RST) models that calculate the components of the Reynolds stress tensor (R) by solving their transport equations.
In comparison to eddy viscosity models (k-epsilon, k-omega), RST models usually are more accurate, but they require larger computational time. They are more accurate because the transport equations regard the effects of streamline curvature, turbulence anisotropy and high strain rates.
Seven equations should be solved (unlike the two equations of K-Epsilon or K-Omega model) and six of them are regarding the Reynolds stresses (symmetric tensor). Therefore, the larger computational time and bigger memory are necessary for this model.

The WALE (Wall-Adapting Local-Eddy Viscosity) Subgrid Scale model is a more modern subgrid scale model that uses a novel form of the velocity gradient tensor in its formulation. Similar to “the Smagorinsky Subgrid Scale model”, it’s negative aspect comes from the limitation that the model coefficient is not universal. But validations using Simcenter STAR-CCM+ have shown that the WALE model is seemingly less sensitive to the value of this coefficient than the Smagorinsky model. Another advantage

of the WALE model is that it does not require any form of near-wall damping, it automatically gives accurate scaling at walls.

3D Quarter model

Firstly, the quarter geometrical model was created imposing an appropriate boundary conditions on the inlet, outlet, walls and also the two symmetries. Then setting all the rest (mesh size, physical conditions, boundary conditions, etc.) RANS model (Linear pressure strain) is simulated up to 1000 iterations where the velocity profile is established and is stable. Then that the physics are changed into LES model (Wale Subgrid Scale) and also the inlet boundary conditions are changed. The fully-developed fluid velocity is characterized by the Reynold's stresses and velocity magnitude. Finally, the simulation proceeded.

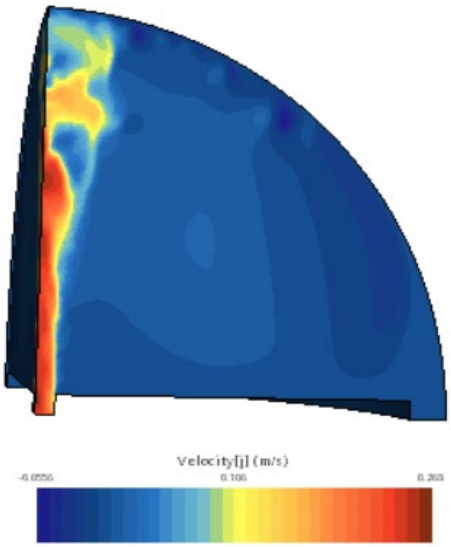

Fig.14: Velocity j-component scene of LES model (Re1, 3D quarter model).

When the results were collected, the data was plotted in order to understand the differences of RANS and LES model and changes during the time.

Unfortunately, the results weren't good enough and in general the vortexes were too high which is not realistic.

It could be due to the fact that two "symmetry" boundary conditions were imposed and it was decided to simulate with 3D full geometry model even if it would be more time consuming simulation.

Full model

New geometry was created and then the physics, mesh size, inlet conditions, etc. were implemented into this full model. Also, new fully-developed fluid velocity was created for this model too, because as geometry changes it is not possible to use the one created for quarter model.

-The base mesh size=2mm

-Volume growth rate=1.0

-Surface growth rate=1.1

So the actual mean mesh size was about 3.3mm and the total number of cells was equal to 943812. The mean mesh size is in the range between Kolmogorov LS and Taylor MS so the full geometry was correctly meshed.

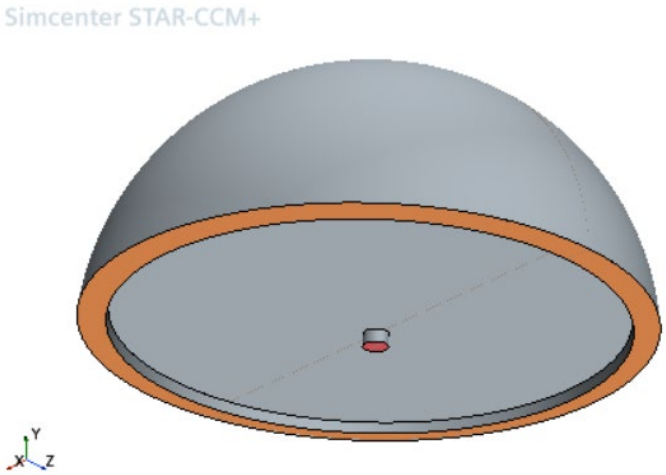

Fig.15: Geometry scene of the full model.

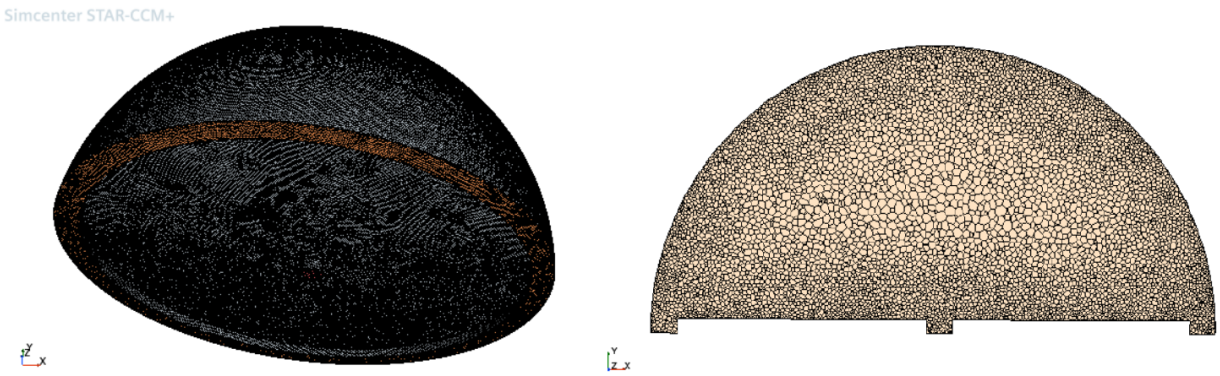

Fig.16: Mesh scene of the full model (a-actual view, b-z plane section view).

Even if the maximum “Convective Courant Number” is close to 1, the mesh size distribution doesn’t seem very appropriate, as it’s bigger where the velocity magnitude is higher. Anyway, it was decided to run the simulation and check the results.

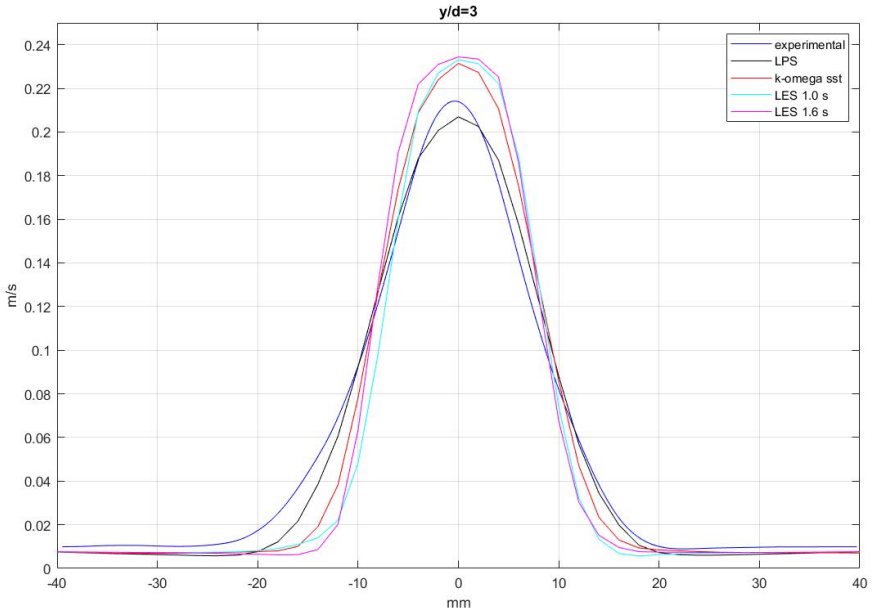

Fig.17: Velocity j-component at y/d=3 (Re1, 3D full model).

At the y/d=3 the RANS (LPS) was very precise to the experimental result which is very good. However, the LES results at two different time are not very unprecise too. At the time 1.0s and 1.6s, the velocity profiles at this distance are almost the same, which means that the shape is almost developed and the flow is stabilized.

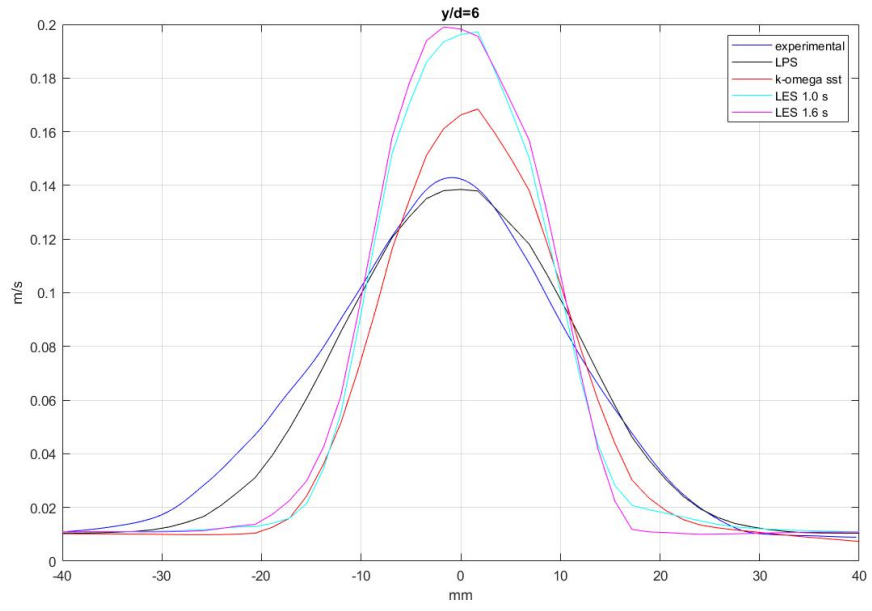

Fig.18: Velocity j-component at y/d=6 (Re1, 3D full model).

However, at the higher distance from the fluid source y/d=6, the LES is moving away from the experimental/actual result. The LES velocity profile was more precise at the y/d=3, though here it has a lower precision. It's noticeable that the LES velocity profiles do not significantly change during the iteration. But LPS is very precise, it is even better than the k-omega sst model.

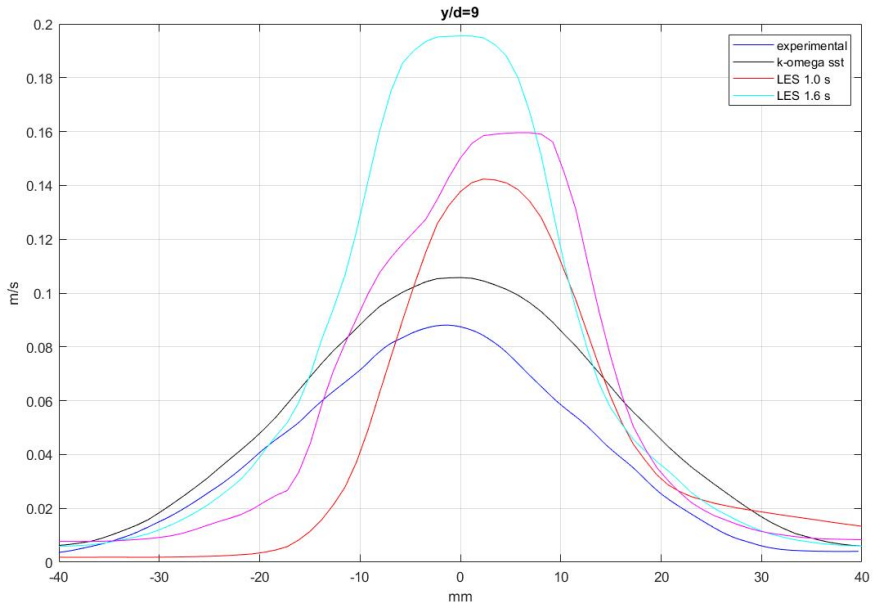

Fig.19: Velocity j-component at y/d=9 (Re1, 3D full model).

At the distance close to the upper plenum (y/d=9), where the velocity shape is not sharp and where it has lower kinetics, LES results differ again from the experimental results and again the LPS model is more precise. K-omega SST fluid flow at high distance begins to move away from the center on xz-plane (inclination of flow).

By comparing and considering the results it was decided:

-To change mesh. Because the RANS model of 3D and 2D were differing a lot. Even if there is an effect of 3D Full model making the profile a bit different from 2D, however it's necessary to check it setting an adaptive mesh with smaller mesh size in the area where the velocity is higher.

-The velocity profiles in LES model are strange and different during the time because of the real time fluctuations and eddies. It is better to obtain a video of the LES in order to understand the flow inside the plenum. Also, the pictures of velocity scene will be taken and studied in this report.

Reduction of base mesh size

First of all, it was tried to set the global base mesh size=1.3mm.

The refined geometry contained: 2900957 cells, 20468423 faces, 17950718 verts. So, it is much finer than it was before and as a result, the computational time increased up to 7. The mesh scene can be seen in the figure below:

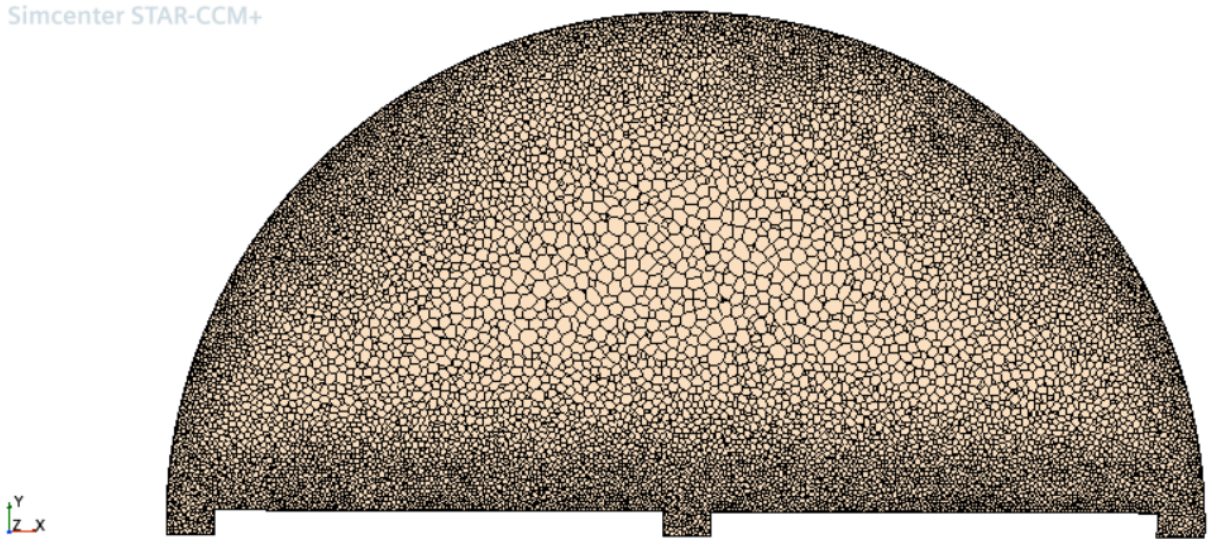

Fig20: mesh scene with mesh base size=1.3[mm] (3D full model).

As it was indicated before, the automatically built mesh does not seem to be effective because the size of mesh is larger near the center of the plenum and considering that the velocity magnitude is higher there, the prediction is that the effect of the decrease of the base mesh size will not be significant. It enlarges while approaching the center due to the fact that it is impossible to set the surface growth rate=1.0. Nevertheless, it was tried to run the simulation and check the obtained results. In the figure below, there is an illustration of the comparison of different RANS models.

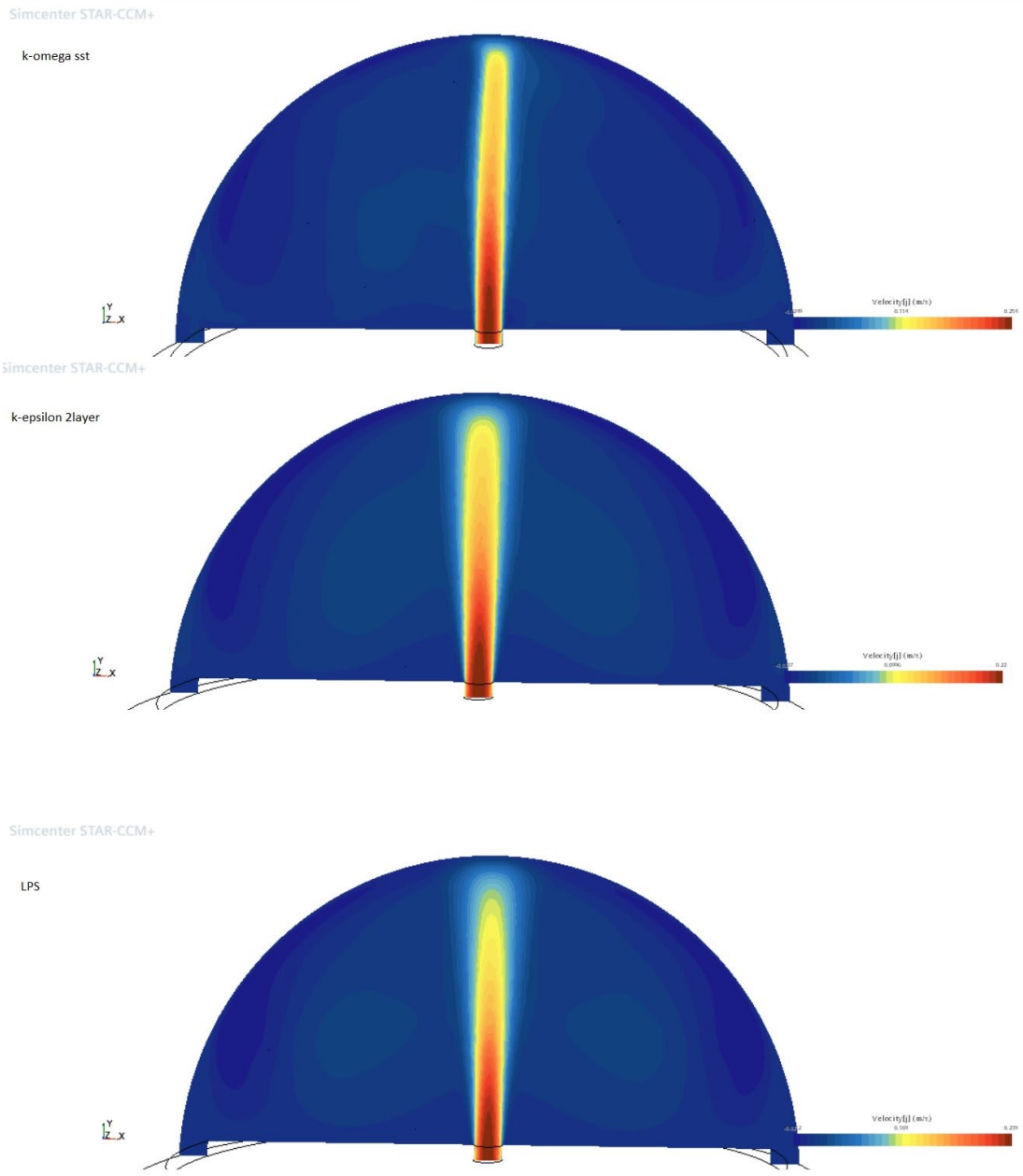

Fig.21: Velocity j-component scenes of RANS models (Re1, 3D full model, mesh size=1.3mm).

The RANS results were the same as they were before (with 3D full model and base size=2mm). Furthermore, the LES results haven't improved too with respect to the previous results with base mesh size=2mm. That is why it was decided to keep the average mesh size around 2mm and decrease it only where it's necessary (where the velocity is higher).

Adapted meshing (Full model)

Base mesh size=2.6mm

-Volume growth rate=1.0

-Surface growth rate=1.05

-Volumetric control. Mesh size inside the cone=1.4mm

The total number of cells is 737271. The mean mesh size was in the range between Kolmogorov LS and Taylor MS so the geometry was correctly meshed.

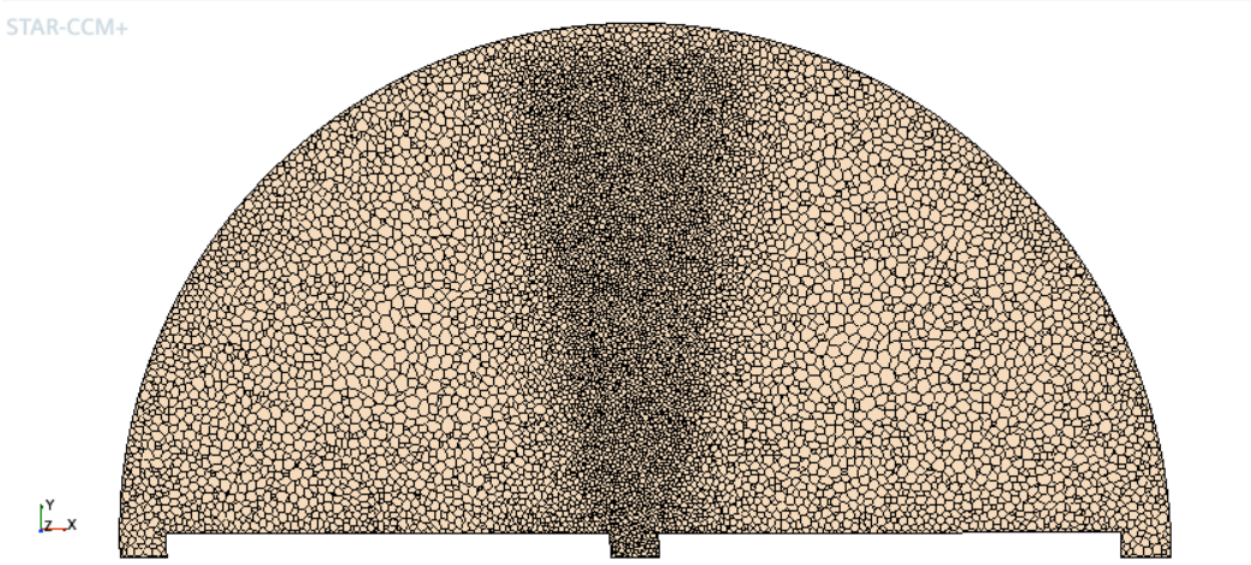

Fig.22: Adapted mesh scene (3D full model).

First of all, three different RANS models (LPS, k-epsilon 2layer, k-omega) were tested with this new mesh, the results can be found in the figure below.

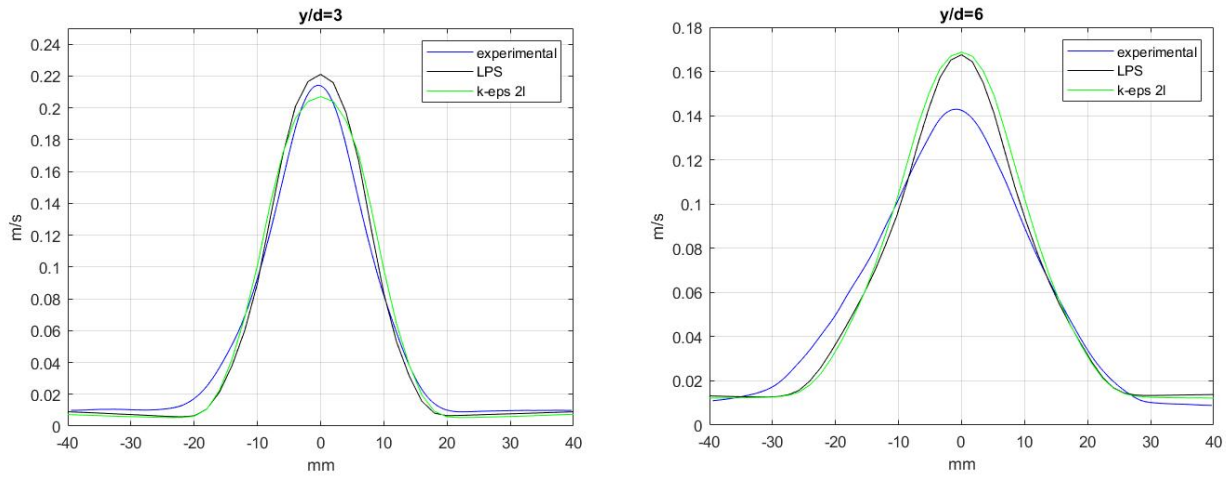

Fig.23: Velocity j-component of RANS models at y/d=3 and y/d=6 (Re1, adapted mesh).

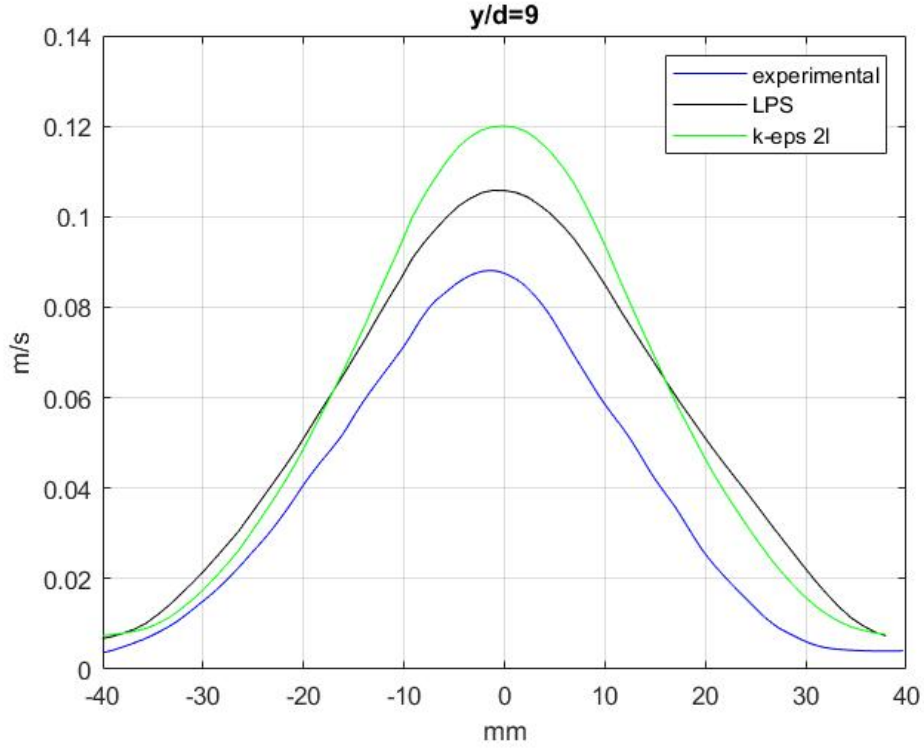

Fig.24: Velocity j-component of RANS models at y/d=9 (Re1, adapted mesh).

The LES model was implemented on the base of developed LPS RANS model. Setting the time step=0.001s and running the simulation for a short time the "Convective courant number" was checked. Taking into account the whole volume of our object, the average courant number is around 1 when the time step=0.15s. But considering the average courant of the whole geometry would be very coarse and even wrong as the velocity of fluid out of center is very small, whereas in the center is high, which makes the central

part very important. So, in order to get the correct results not only in the sides of the geometry but also in the center, it's necessary to make the convective courant number in the central part equal to 1, which dramatically decreases the time step. To be sure and secure, it was decided to keep the maximum courant number around 1, which sets the time step=0.001s.

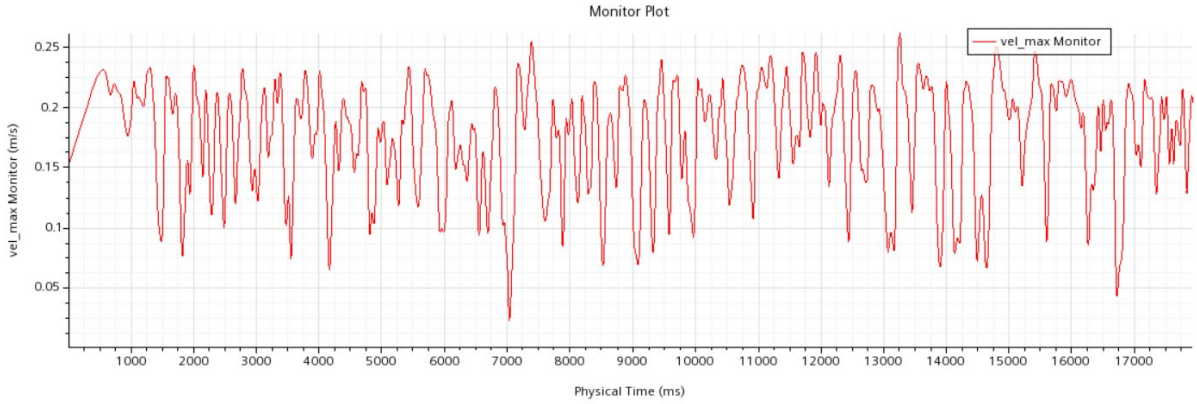

Fig.25: Monitoring of the velocity magnitude at the point probe (Re1, adapted mesh).

The point probe around the center of the geometry shows how much the velocity oscillates, this is what actually happens when the "LES Wale Subgrid" model is implemented. The amplitude of oscillations is quite significant and the frequency is quite high. That is why it was decided to extract the velocity components each 0.02s in order to catch the contribution of such oscillations.

But in order to see the general trend of velocity, the point probe data, statistically averaged in time, was considered. The monitor plot is below:

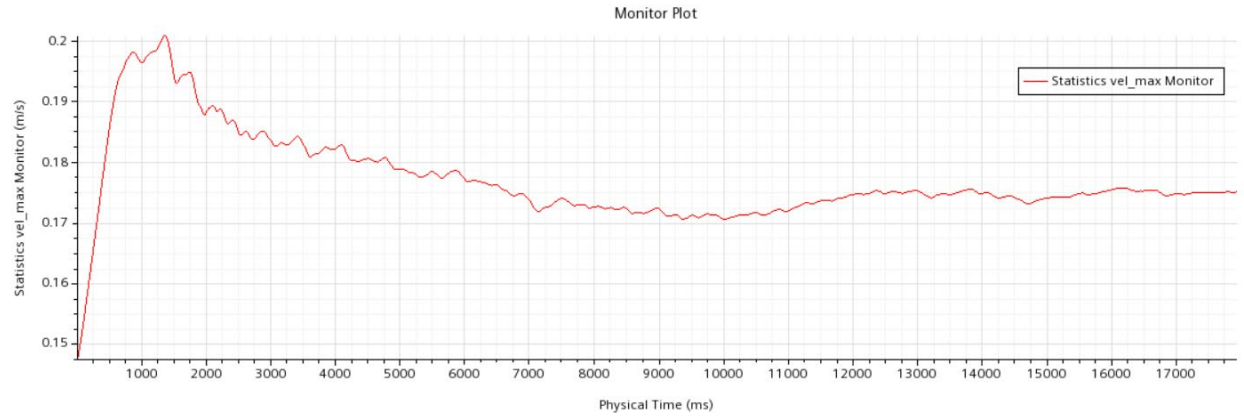

Fig.26: Trend of the velocity magnitude at the point probe (Re1, adapted mesh).

The plot shows that the stabilization has begun starting from around 1.5 seconds which lasted about 6 seconds. Starting from 12 seconds the j-component (main) of the fluid flow becomes much more stable, but anyway, there is some presence of little changes.

Some results can be seen also in a form of a scene. The j-component scenes of the fluid flow captured in the time period between 6.2-7.2 seconds is below:

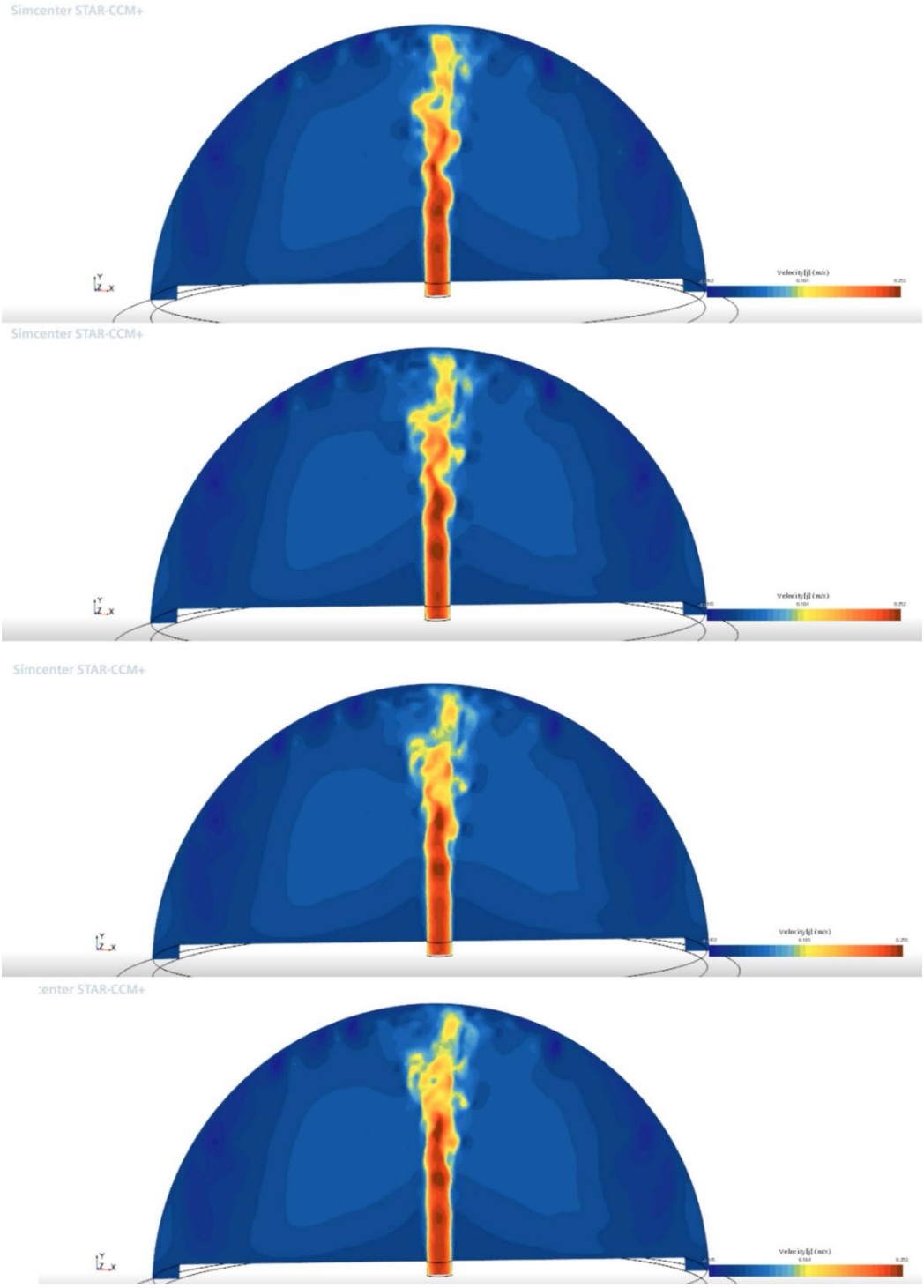

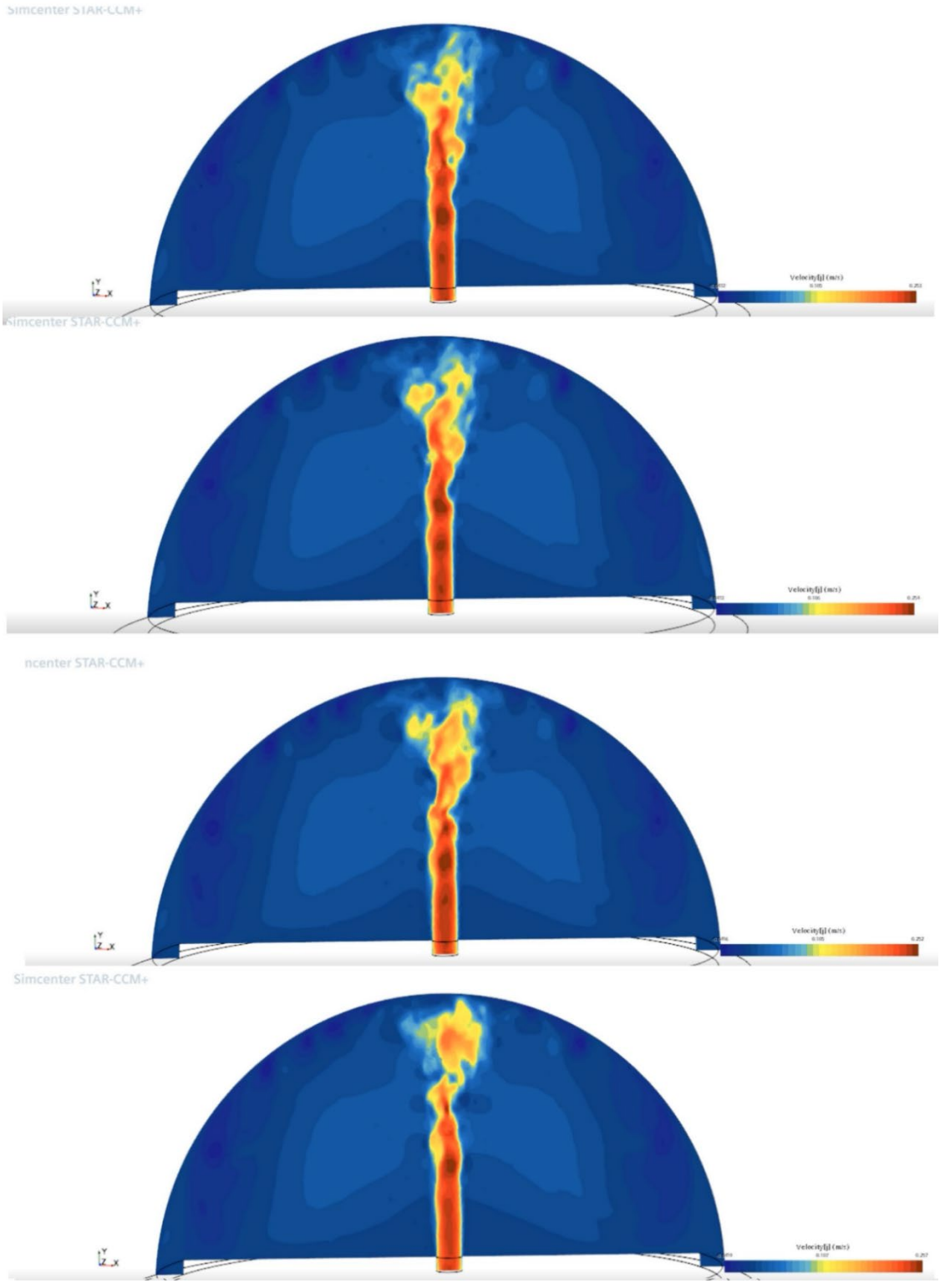

Fig.27a, 27b: Velocity j-component scenes of LES model in the time period between 6.2-7.2[s] (Re1, adapted mesh).

Looking at these scenes it is understandable that the instantaneous captures of velocity profile at different height is not effective because it is a transient state. So it was decided to take four line probes at different height levels (3d, 6d, 9d).

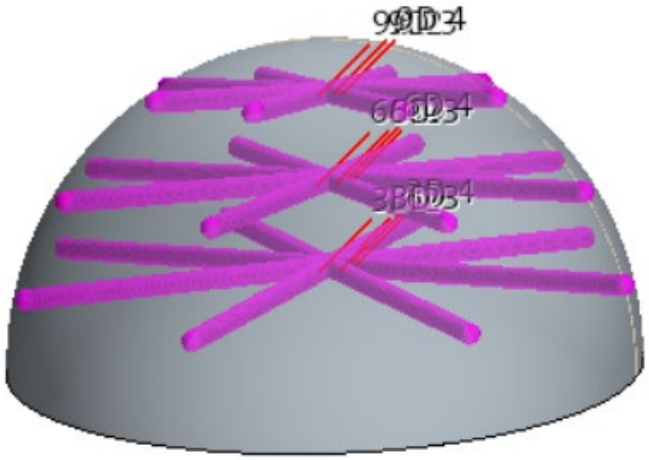

Fig.28: Geometry scene with the line probes.

The collected data was averaged in time by superimposing the velocity components at each dt, considering the position in space (x,y,z) related to each velocity component. Then in order to average this data in space it was compulsory to pass from cartesian into cylindrical (polar) coordinates, otherwise it would have been difficult to handle the data from the lines probes that don't lie on the xy or zy planes.

```
85 -    d49=sortrows(d49,3); d50=sortrows(d50,3);
86
87      %x,z,y --> theta,r,y (without velocity)
88 -    [dp1(:,1),dp1(:,2),dp1(:,3)]=cart2pol(d1(:,2),d1(:,4),d1(:,3));
89 -    [dp2(:,1),dp2(:,2),dp2(:,3)]=cart2pol(d2(:,2),d2(:,4),d2(:,3));
90 -    [dp3(:,1),dp3(:,2),dp3(:,3)]=cart2pol(d3(:,2),d3(:,4),d3(:,3));
91 -    [dp4(:,1),dp4(:,2),dp4(:,3)]=cart2pol(d4(:,2),d4(:,4),d4(:,3));
92 -    [dp5(:,1),dp5(:,2),dp5(:,3)]=cart2pol(d5(:,2),d5(:,4),d5(:,3));
93 -    [dp6(:,1),dp6(:,2),dp6(:,3)]=cart2pol(d6(:,2),d6(:,4),d6(:,3));
94 -    [dp7(:,1),dp7(:,2),dp7(:,3)]=cart2pol(d7(:,2),d7(:,4),d7(:,3));
95 -    [dp8(:,1),dp8(:,2),dp8(:,3)]=cart2pol(d8(:,2),d8(:,4),d8(:,3));
96 -    [dp9(:,1),dp9(:,2),dp9(:,3)]=cart2pol(d9(:,2),d9(:,4),d9(:,3));
97 -    [dp10(:,1),dp10(:,2),dp10(:,3)]=cart2pol(d10(:,2),d10(:,4),d10(:,3));
98 -    [dp11(:,1),dp11(:,2),dp11(:,3)]=cart2pol(d11(:,2),d11(:,4),d11(:,3));
99 -    [dp12(:,1),dp12(:,2),dp12(:,3)]=cart2pol(d12(:,2),d12(:,4),d12(:,3));
100 -   [dp13(:,1),dp13(:,2),dp13(:,3)]=cart2pol(d13(:,2),d13(:,4),d13(:,3));
101 -   [dp14(:,1),dp14(:,2),dp14(:,3)]=cart2pol(d14(:,2),d14(:,4),d14(:,3));
102 -   [dp15(:,1),dp15(:,2),dp15(:,3)]=cart2pol(d15(:,2),d15(:,4),d15(:,3));
103 -   [dp16(:,1),dp16(:,2),dp16(:,3)]=cart2pol(d16(:,2),d16(:,4),d16(:,3));
104 -   [dp17(:,1),dp17(:,2),dp17(:,3)]=cart2pol(d17(:,2),d17(:,4),d17(:,3));
105 -   [dp18(:,1),dp18(:,2),dp18(:,3)]=cart2pol(d18(:,2),d18(:,4),d18(:,3));
```

Fig.29: Matlab script to sort the data.

R (m)	Y (m)	Velocity (j) (m/s)
0	0.05715	0.225809364
0.002	0.05715	0.217277756
0.002	0.05715	0.235379417
0.002	0.05715	0.23112706
0.002	0.05715	0.223591407
0.002001112	0.05715	0.223980129
0.002001112	0.05715	0.232752912
0.002001112	0.05715	0.217340776
0.002001112	0.05715	0.236283507
0.004	0.05715	0.186745387
0.004	0.05715	0.228718763
0.004	0.05715	0.230111211
0.004	0.05715	0.209928144
0.004002224	0.05715	0.209319537
0.004002224	0.05715	0.226149409

Table2: Example of the sorted data.

The definitive file is sorted by height, angle and also by radius. There are 3 levels of height, each containing 793 rows and in total, the file contains 2395 rows. In each row range, which is related to special height, the radius is sorted from zero to the maximum. In the table 2 it is shown that there are four different velocity j-components referring the same radius. The is due to the fact that each radius refers to corresponding angle. Later on, the opposite located data (in terms of angle) will be collected in order to plot the velocity shapes.

Finally, the data have been averaged also in space. Now it is possible to compare the velocity shapes of the different models corresponding to different height levels.

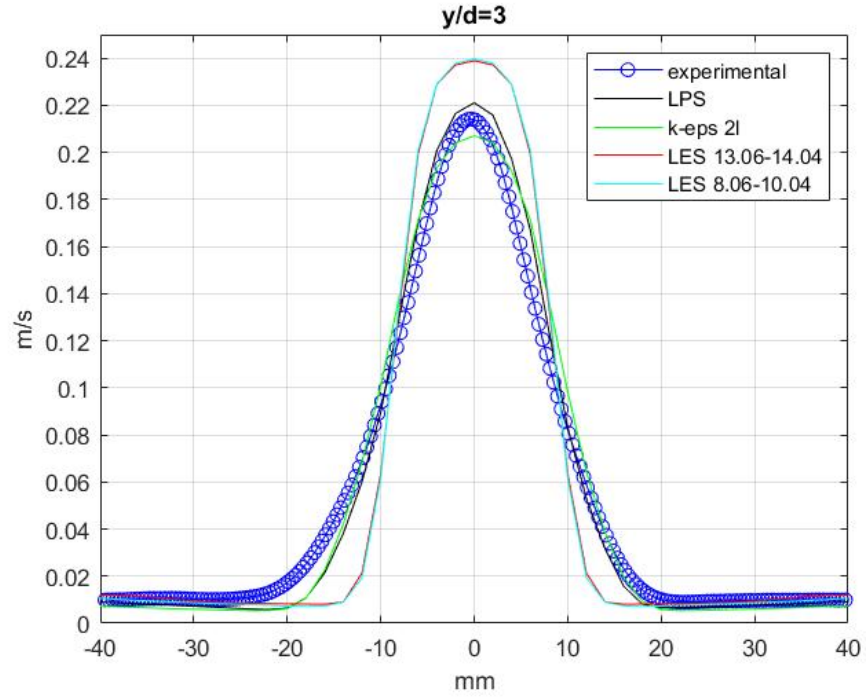

Fig.30: Velocity j-component at y/d=3 (Re1, adapted mesh).

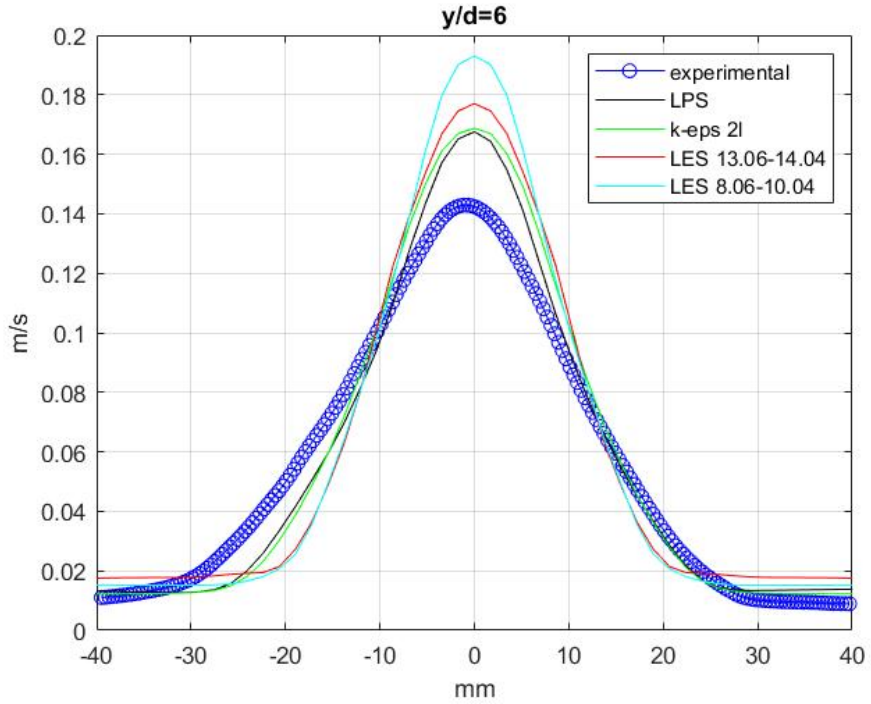

Fig.31: Velocity j-component at y/d=6 (Re1, adapted mesh).

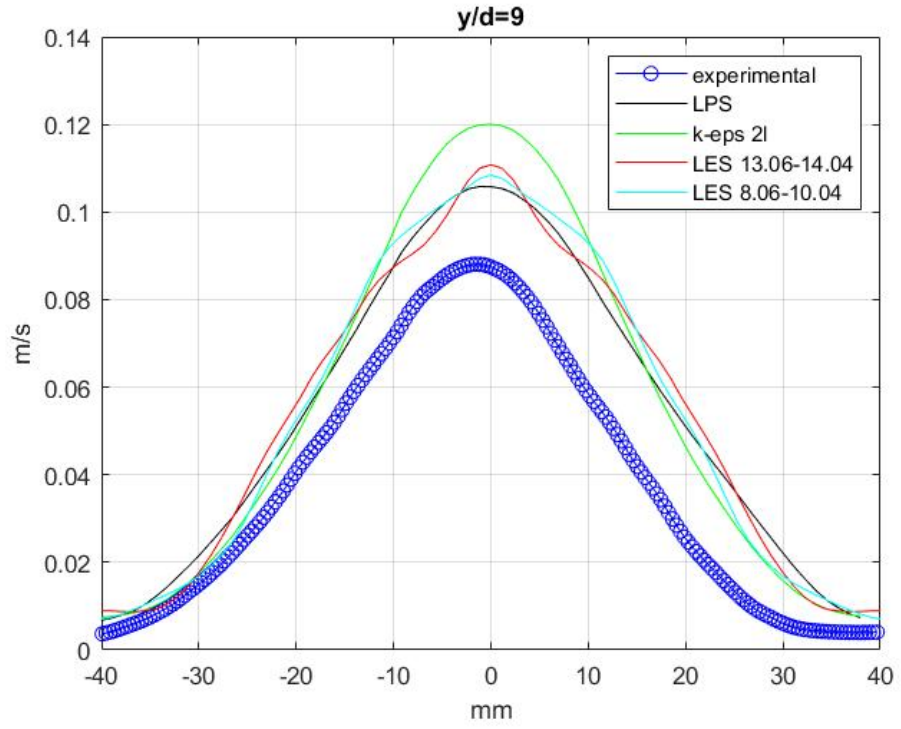

Fig.32: Velocity j-component at y/d=9 (Re1, adapted mesh).

The obtained LES results are similar to RANS results except the one at the distance 3d from the inlet. The initial turbulence and velocity of the fluid seems to be overestimated at the region which is close to the inlet boundary condition. At the distance 6d, there is a significant difference between two LES results, even if they are not instantaneous results, but the averaged in time and space over few seconds (considering 50 captured data each second). This is mostly due to the fact that the flow is better stabilized starting from 12 seconds (ref. to fig.23).

In order to enhance it, it was tried to slightly change the inlet boundary conditions. Before, the fluid was mainly described by initial Reynold's stresses with length scale, where the length scale was defined manually by taking the average of Kolmogorov's LS and Taylor's MS throughout the geometry. Now it will be tried to define the developed fluid by the intensity. Taking into account the fact that the intensity of fluid wave is the average power that travels through an area as the wave travels through space, it's predicted that this boundary condition will improve the results, mostly near the inlet.

Having changed the inlet boundary conditions and consequently the fully-developed fluid, the new simulation has been run.

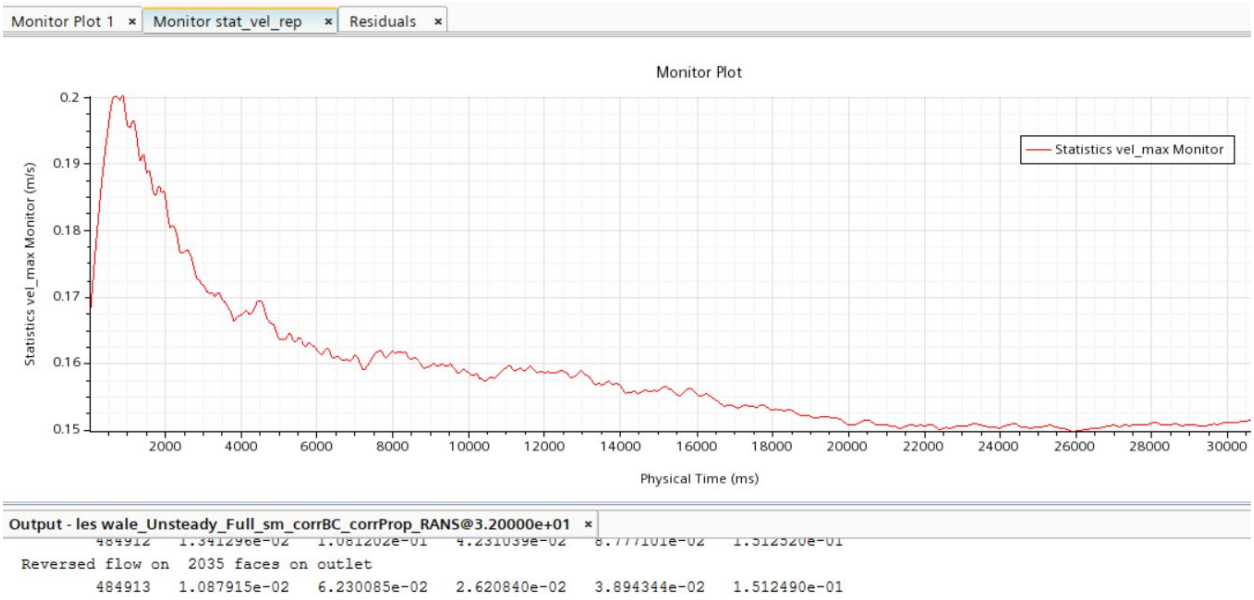

Fig.33: Trend of the velocity magnitude at the point probe (Re1, adapted mesh, Intensity+Length scale).

As predicted, the statistically averaged velocity at the point probe was lower than the velocity in the previous simulation. And consequently, the results of velocity j-component should be also lower. The slope of stabilization trend decreased starting from 8 seconds, but the fluid flow became much more stabilized starting from 20 seconds. The velocity j-components were analyzed and compared in different time range.

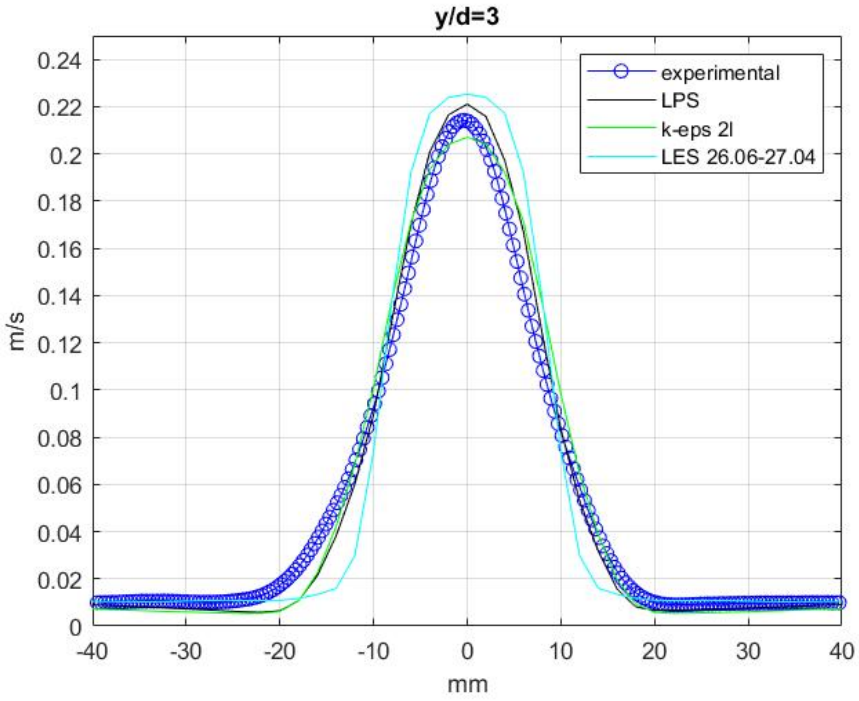

Fig.34: Velocity j-component at y/d=3 (Re1, adapted mesh, Intensity+Length scale).

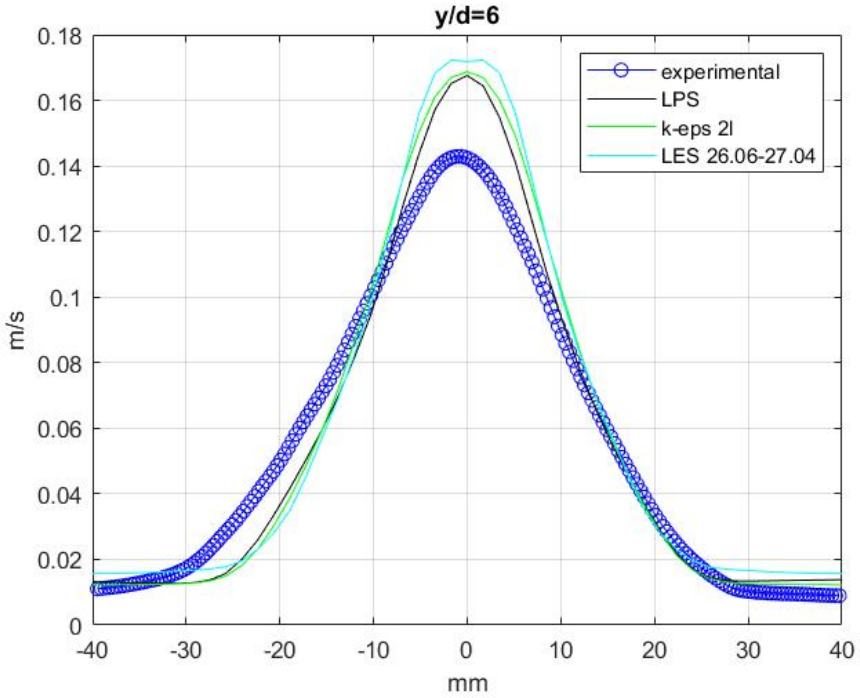

Fig.35: Velocity j-component at y/d=6 (Re1, adapted mesh, Intensity+Length scale).

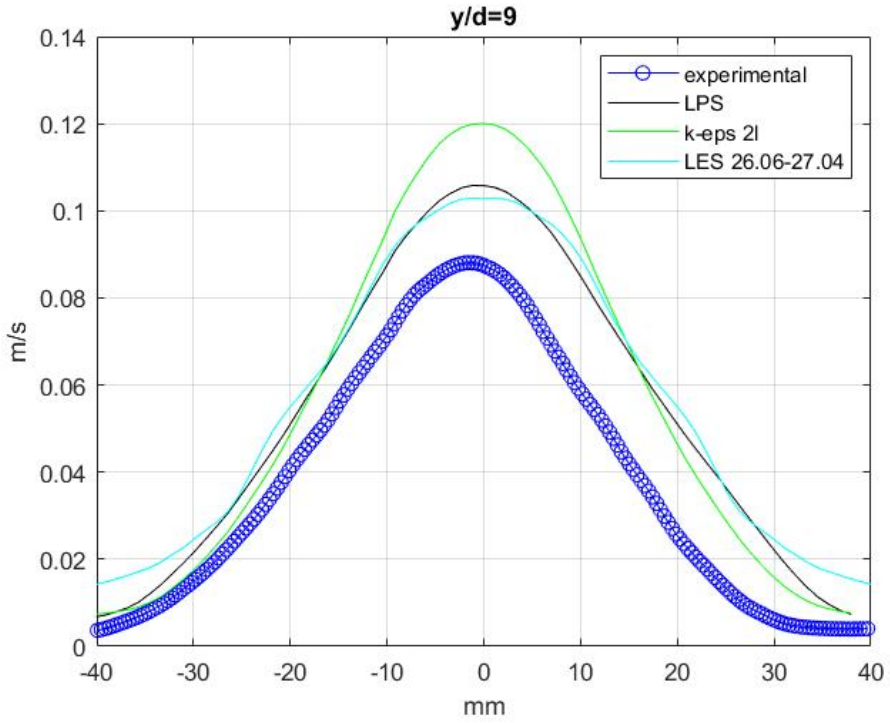

Fig.36: Velocity j-component at y/d=9 (Re1, adapted mesh, Intensity+Length scale).

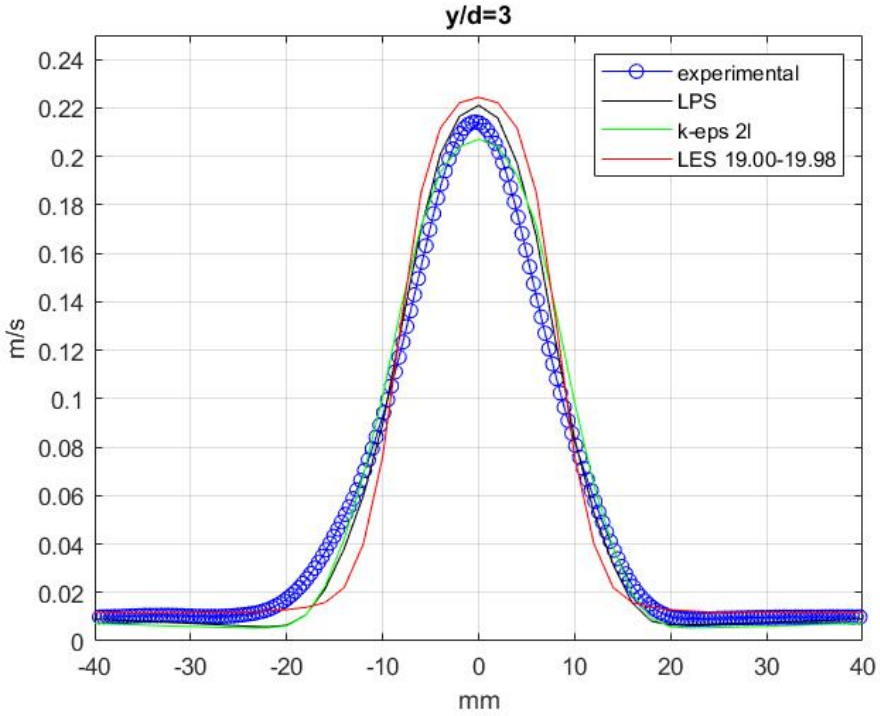

Fig.37: Velocity j-component at y/d=3 (Re1, adapted mesh, Intensity+Length scale).

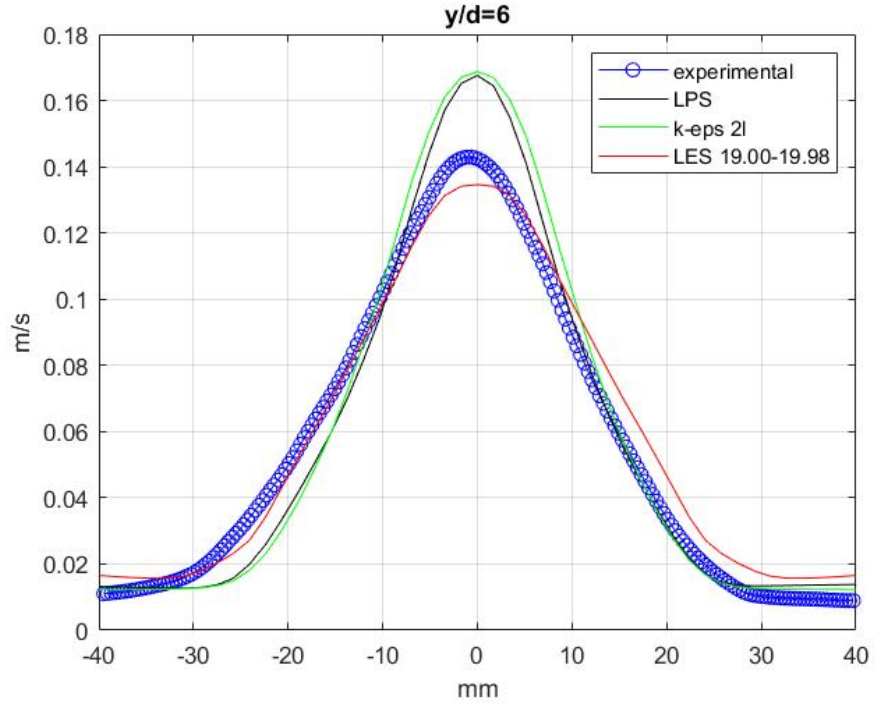

Fig.38: Velocity j-component at y/d=6 (Re1, adapted mesh, Intensity+Length scale).

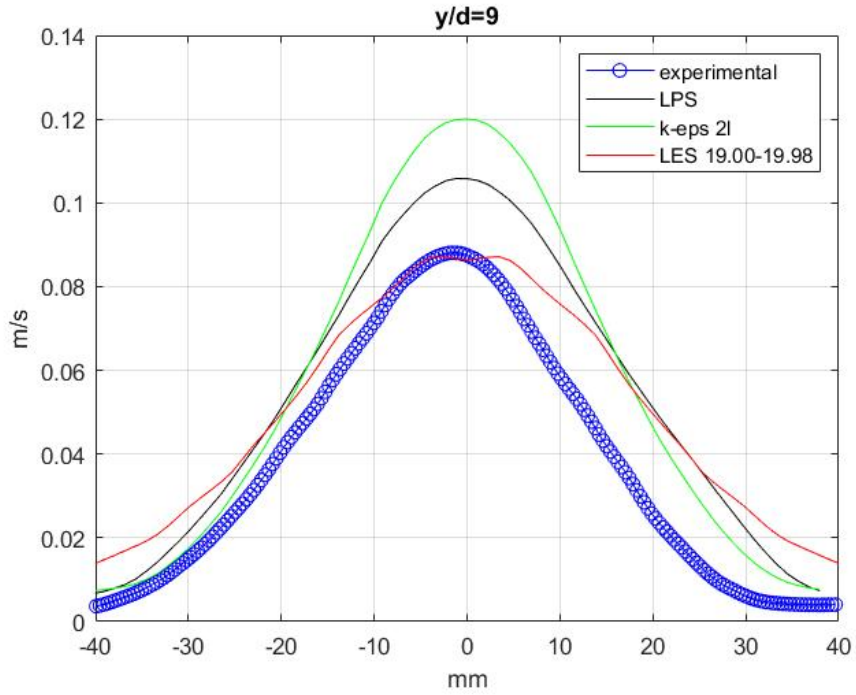

Fig.39: Velocity j-component at y/d=9 (Re1, adapted mesh, Intensity+Length scale).

Despite the new obtained results were much better than RANS models or LES models with previous boundary conditions, the simulation was run further to see whether there will be the convergence or whether the stability will be hold.

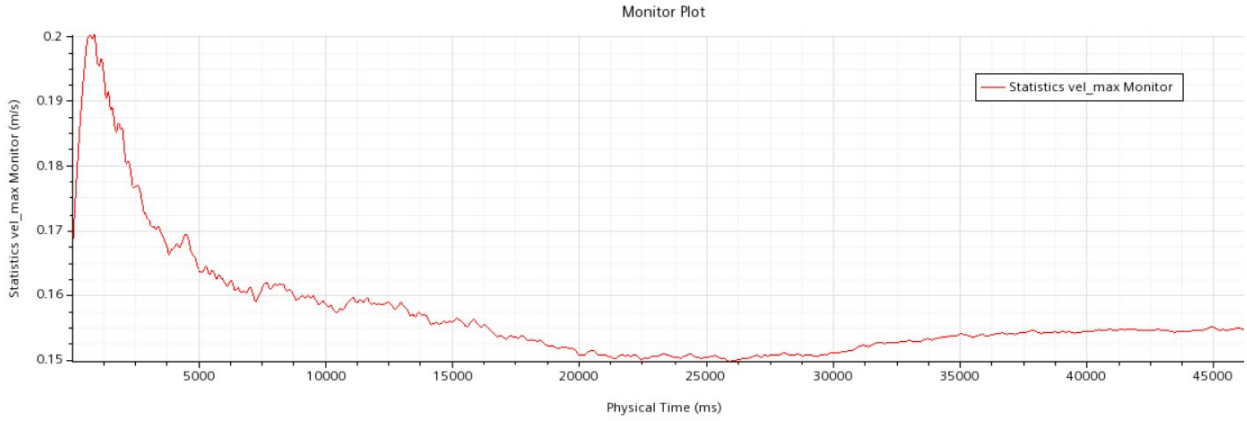

Fig.40: Trend of the velocity magnitude at the point probe (Re1, adapted mesh, Intensity+Length scale).

Looking at the trend of velocity magnitude monitor, it can be understood that the actual stability occurs starting from 35 seconds. Even if the convergence is less than the one in the time range 20-30 seconds, the results are probably better that will be checked. It could be compared with the recent most appropriate LES result.

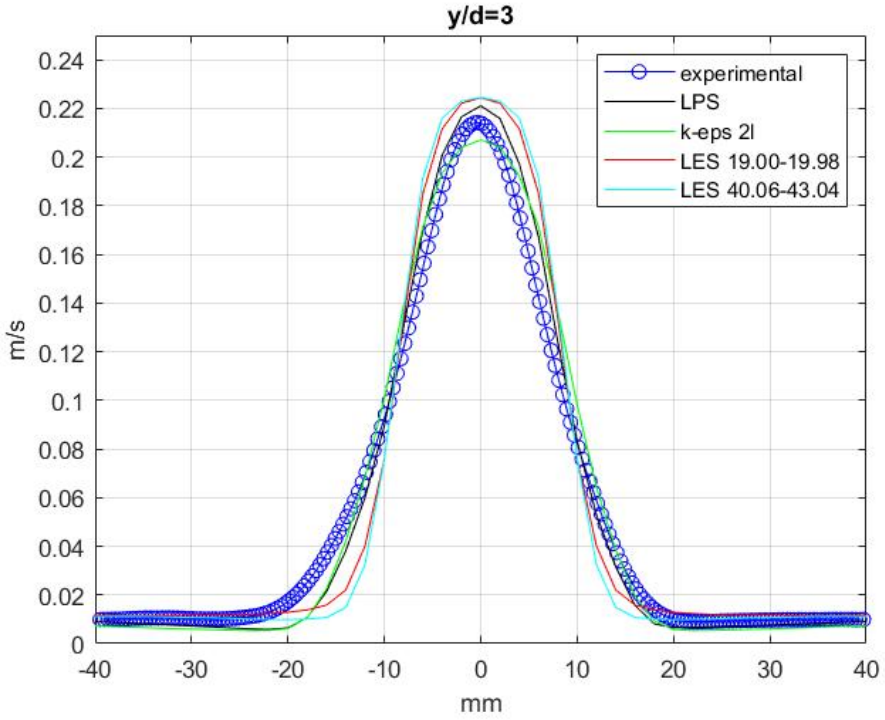

Fig.41: Velocity j-component at y/d=3 (Re1, adapted mesh, Intensity+Length scale).

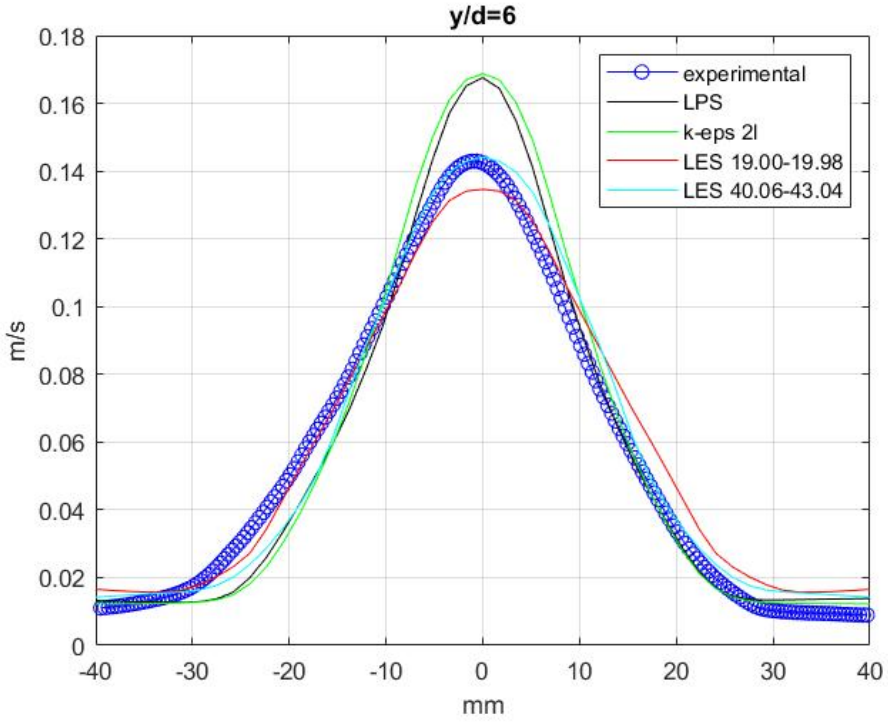

Fig.42: Velocity j-component at y/d=6 (Re1, adapted mesh, Intensity+Length scale).

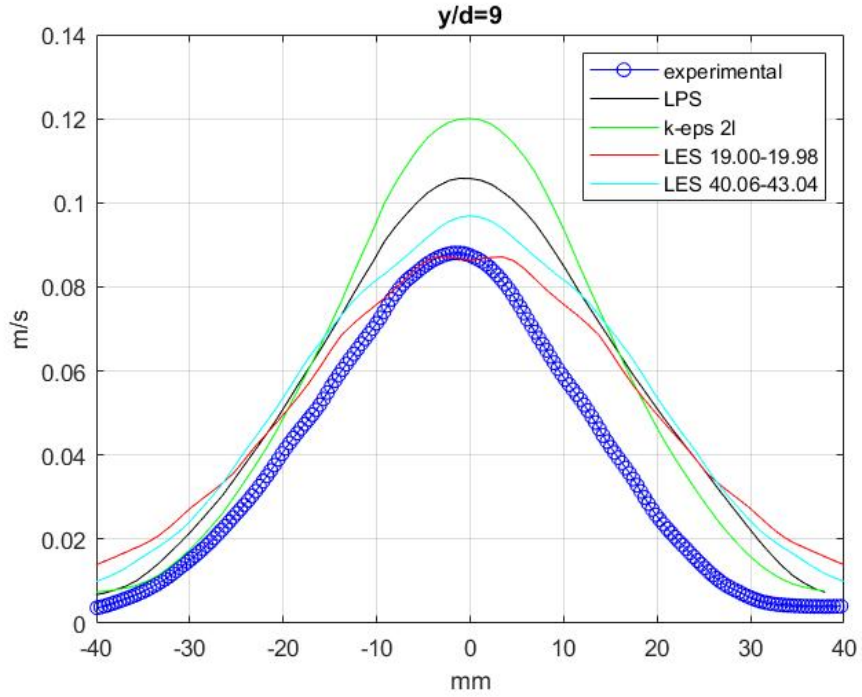

Fig.43: Velocity j-component at y/d=9 (Re1, adapted mesh, Intensity+Length scale).

In general, that last changes concerning the inlet boundary conditions have improved the results obtained by Wale Subgrid Scale (LES) model. In the plots above, it is illustrated that in some time range the results are comparable with those of RANS models while in another time range they are even more precise, considering that in LES model the process is transient. Moreover, the velocity j-component close to the inlet at the distance 3d has been improved almost in the entire time range of the new simulation.

i-component

Having achieved good results of the main component (j-component) of fluid velocity, it would be reasonable to check and compare also other components of the turbulent fluid. As i-components and k-components are perpendicular but located on the same xz-plane, it would be reasonable if only the i-components will be plotted and compared. It was simulated on the last and most appropriate model with an adapted mesh having delta t=0.02s.

In order to be consistent with the j-components analysis, it was decided to plot the averaged results in the time range between 26.06-27.04[s].

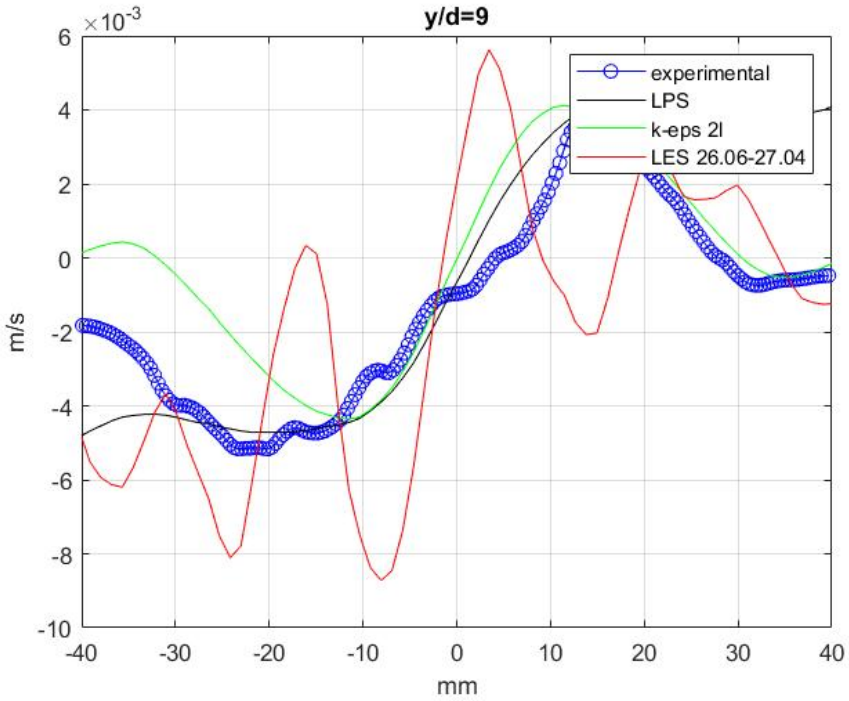

Fig.44: Velocity i-component at y/d=9 (zoomed) (Re1, adapted mesh, LES 26.06-27.04).

The results of LES at the distance 3d is comparable with the RANS k-epsilon 2 layer results, while the Linear Pressure Strain model is less precise, however, zooming out the plot of results at 3d, the high oscillations can be noticed. The same situation happens at the higher distance of 9d, where the error is similar to the aliasing error from the signal theory. And indeed, it seems that this error occurs due to the fact that horizontal velocities (i-component and k-component) consist of fluctuations with higher frequency, thus it was important to decrease the delta time at which the velocity components were captured. As an alternative, it is also feasable to consider the LES results in a larger time range. Therefore, the i-components of velocity in the time range between 26.06-29.04 was considered and averaged in time and space. The results can be seen in the following figures:

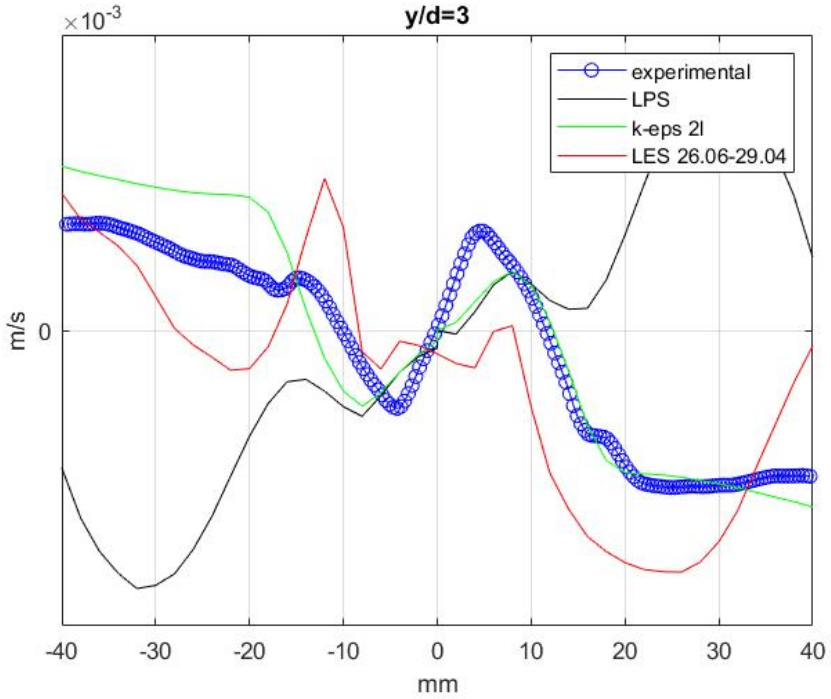

Fig.45: Velocity i-component at y/d=3 (zoomed) (Re1, adapted mesh, LES 26.06-29.04).

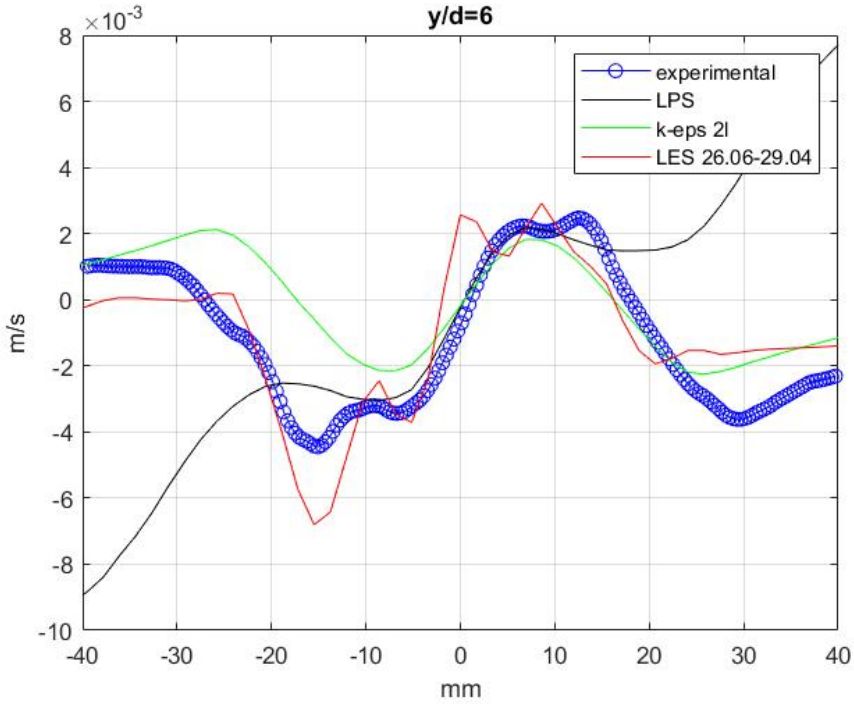

Fig.46: Velocity i-component at y/d=6 (zoomed) (Re1, adapted mesh, LES 26.06-29.04).

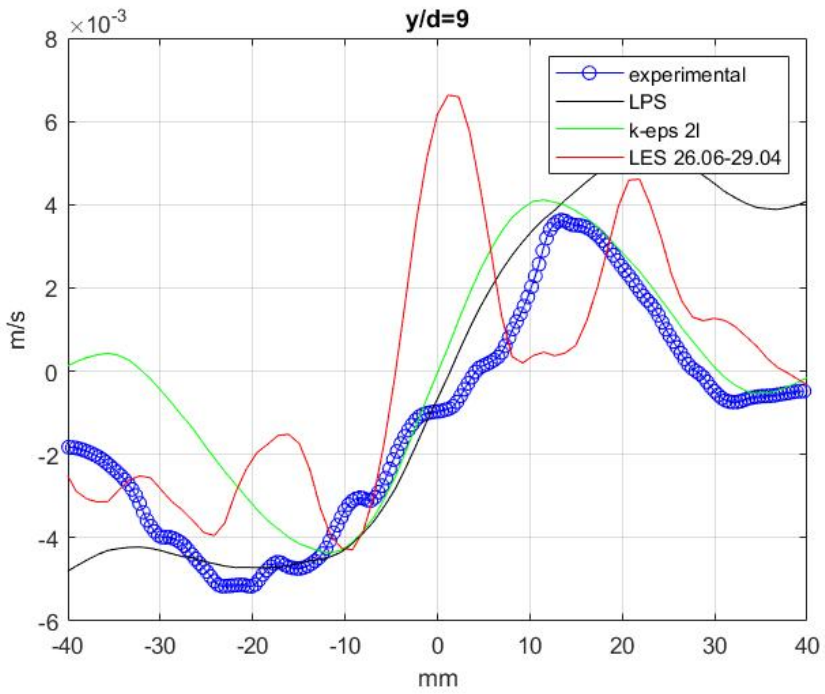

Fig.47: Velocity i-component at y/d=9 (zoomed) (Re1, adapted mesh, LES 26.06-29.04).

The plots of i-component of larger time range is much precise than previous LES result that were averaged in the time range of one second at the 3d and 6d distances, however the effect of fluctuation partly remains at the distance of 9d even if it has become much better.

In order to obtain better i-component LES result at the 9d height level from the inlet, it was decided to change the capture delta time of velocity components to 0.005[s], which is four times smaller than it was before. For comparison: if only fifty fluid velocity data (components, position) were averaged in one second before, having delta t=0.005[s], there will be two hundred velocity data averaged in one second now.

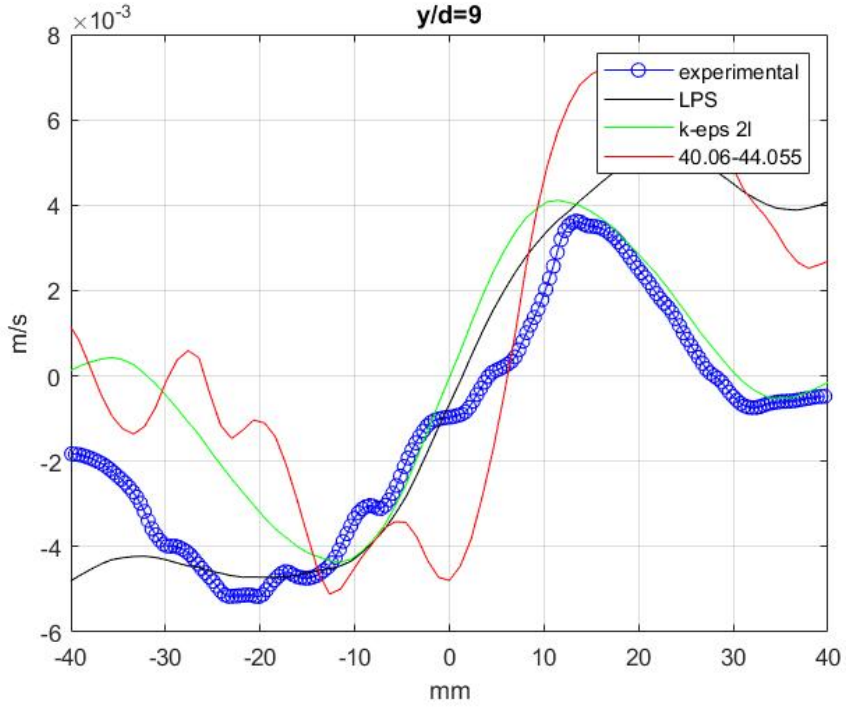

Fig.48: Velocity i-component at y/d=9 (zoomed) (Re1, adapted mesh, LES 40.06-44.005, dt=0.005s).

Finally, as it was assumed, with the decrease of delta time and increase of the time range on which the velocity components were captured, the amplitude of fluctuations are indeed decreased and the overall result has become more precise even near the upper plenum.

Conclusion

During this thesis work different models and approaches were tried and implemented which consequently led to diverse results. In the beginning, the several RANS models were used in the simulation and results demonstrated that they can be pretty precise and sufficiently reliable if the initial conditions, boundary conditions, mesh size and distribution were set correctly. Although the RANS models are simple and do not require high computational rate and large computational time, the initial conditions can have dramatic effect on the final results, for example: even a 1 degree of temperature difference will change the viscosity of the fluid and also some other less important parameters, leading to the results which differ more from the experimental data so that the initial condition is not adequate anymore. Situation is much more complicated with

the boundary conditions, because there is no data which can be considered as ultimately correct, that is why here several approaches can be considered. With the trial and verification procedure the more suitable boundary conditions can be chosen, although having a good knowledge of fluid dynamics, physics of turbulent flow at different Reynold's number or just a considerable experience, can save much time to choose the correct boundary conditions.

The LES model is much more complicated not only in the terms of the numerical solution and consequently computational time, but also in terms of preparation of feasible parameters and settings for the model. During the work it was observed and discovered that meshing parameters and delta time can be considered as key factors of the results. Being a transient process, it involves more field functions and some of them can help to understand the validity of the model, including mesh sizing and determination of the time step. Moreover, it would be much helpful to set some appropriate monitors which can also help to estimate the validity of the transient model and in case of necessity to motivate to make some changes in order to obtain better results. Through multiple trials and errors, finally, it has come up to the point that in the case that all the initial settings are set in a correct way, by Wale Subgrid Scale (LES) model, it is possible to obtain very precise results which can be very useful in the design of a cooling system of the 4^{th} generation fission reactors.

References

1) Alwafi, A., Nguyen, T., Anand, N. and Hassan, Y. (2018). Time-resolved particle image velocimetry measurements and proper orthogonal decomposition analysis of jet impingement in a HTGR upper plenum, *Transactions of the American Nuclear Society* 118: 1120–1122.

2) Experimental Modeling of VHTR Plenum Flows During Normal Operation and Pressurized Conduction Cooldown INL/EXT-06-11760. Glenn E. McCreery, Keith G. Condie.

3) Simulation software: Simcenter STAR-CCM+ 2021.2 (16.04.007-R8).

4) Jones, W.P., and Launder, B.E. 1972. "The Prediction of Laminarization with a Two-Equation Model of Turbulence", Int. J. Heat and Mass Transfer, 15, pp. 301-314.
5) Menter, F.R. 1994. "Two-equation eddy-viscosity turbulence modeling for engineering applications", AIAA Journal, 32(8), pp. 1598-1605.

6) Shih, T.-H., Liou, W.W., Shabbir, A., Yang, Z. and Zhu, J. 1994. "A New k-epsilon Eddy Viscosity Model for High Reynolds Number Turbulent Flows -- Model Development and Validation", NASA TM 106721.

7) Gibson, M.M. and Launder, B.E. 1978. "Ground effects on pressure fluctuations in the atmospheric boundary layer", J. Fluid Mech., 86(3), pp. 491-511.

8) Setup of LES useful guidelines: https://docs.sw.siemens.com/documentation/external/PL20200227072959152/en-US/userManual/userGuide/html/index.html#page/STARCCMP%2FGUID-51C6C100-2DC6-4DDA-BD49-E59A402AF540.html%23

9) Nicoud, F. and Ducros, F., 1999. "Subgrid-Scale Stress Modelling Based on the Square of the Velocity Gradient Tensor," Flow, Turbulence and Combustion, 62, pp. 183-200.